

Benchmarking and Learning Multi-Dimensional Quality Evaluator for Text-to-3D Generation

Yujie Zhang^{1*} Bingyang Cui^{1*} Qi Yang² Zhu Li² Yiling Xu^{1†}

¹ Shanghai Jiao Tong University ² University of Missouri-Kansas City

¹{yujie19981026, cccby0813, yl.xu}@sjtu.edu.cn , ²{qiyang, lizhu}@umkc.edu

Abstract

Text-to-3D generation has achieved remarkable progress in recent years, yet evaluating these methods remains challenging for two reasons: i) Existing benchmarks lack fine-grained evaluation on different prompt categories and evaluation dimensions. ii) Previous evaluation metrics only focus on a single aspect (e.g., text-3D alignment) and fail to perform multi-dimensional quality assessment. To address these problems, we first propose a comprehensive benchmark named MATE-3D. The benchmark contains eight well-designed prompt categories that cover single and multiple object generation, resulting in 1,280 generated textured meshes. We have conducted a large-scale subjective experiment from four different evaluation dimensions and collected 107,520 annotations, followed by detailed analyses of the results. Based on MATE-3D, we propose a novel quality evaluator named HyperScore. Utilizing hypernetwork to generate specified mapping functions for each evaluation dimension, our metric can effectively perform multi-dimensional quality assessment. HyperScore presents superior performance over existing metrics on MATE-3D, making it a promising metric for assessing and improving text-to-3D generation. The project is available at <https://mate-3d.github.io/>.

1. Introduction

Remarkable advances in text-to-3D generative methods have been witnessed in recent years [31]. Given textual descriptions (*i.e.*, prompts), these methods have the capability to generate contextually relevant 3D representations, such as textured mesh [53], Neural Radiance Field (NeRF) [13, 19, 38], and 3D Gaussian Splatting (3DGS) [23, 46, 52, 65]. Unlike traditional distortions in 3D data processing (*e.g.*, noise, lossy compression), generated 3D

* Equal Contribution.

† Corresponding Author.

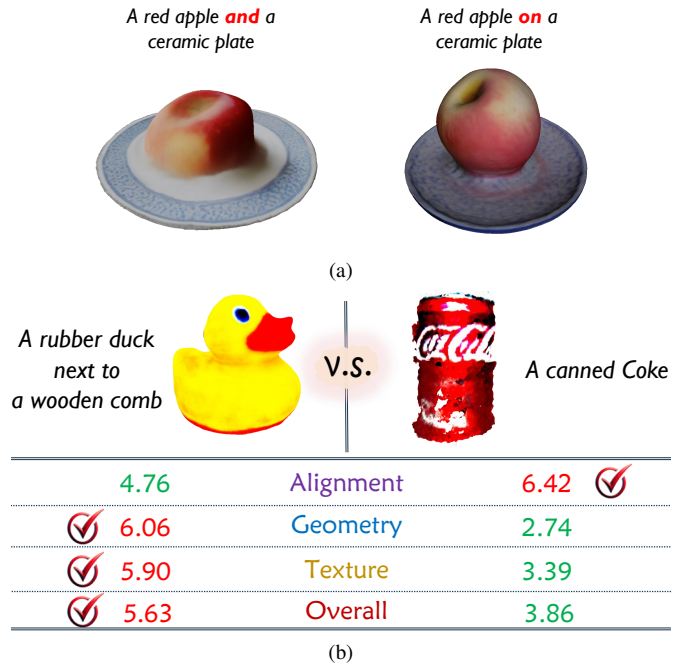


Figure 1. (a) Diverse generation results from similar prompts. (b) Quality evaluation from multiple perspectives.

representations may suffer from some unique degradations, such as misalignment with prompt semantics and multi-view inconsistency (*i.e.*, the Janus problem) [16, 42]. To better guide the method design and support fair comparisons, it is important to explore subjective-aligned quality evaluation for text-to-3D generation methods.

Previous works have conducted text-to-3D evaluation by proposing new benchmarks. For example, T³Bench [12] constructs three prompt classes with increasing scene complexity, including *Single object*, *Single object with surroundings*, and *Multiple objects*, followed by collecting 630 texture meshes annotated from two dimensions, *i.e.*, quality and alignment. However, these benchmarks have two main drawbacks. i) **Lack of Prompt Diversity**. Although these

benchmarks [12, 20, 58] have classified prompts based on textual complexity or object quantity, their categorization generally lacks an adequate degree of distinction. In fact, we observe that some similar prompts usually lead to visually different results, as shown in Fig. 1a. Therefore, a more fine-grained categorization is essential to gain a comprehensive understanding of model capabilities. ii) **Limited Evaluation Dimension.** As shown in Fig. 1b, the overall quality of the generated 3D representation is influenced by different factors, including geometry fidelity, texture details, and text-3D alignment. A single score is insufficient to perform detailed comparison between different cases. Consequently, it is necessary to construct a comprehensive benchmark with higher prompt diversity and richer evaluation dimensions.

Another challenge in text-to-3D evaluation is the lack of accurate and automated metrics to assess the quality of generated results. Existing approaches [57] rely primarily on subjective user studies, which are constrained by high costs in terms of time, money, and rigorous testing environment. Some previous work [39, 53, 61] has attempted to address this by rendering the 3D objects into single or multiple 2D images and using CLIP- [43] or BLIP- [27] based metrics [14, 47, 59, 62] to measure the alignment between the prompts and the rendered images. However, these metrics focus on the text-3D correspondence, ignoring other critical aspects of subjective perception, such as geometry and texture fidelity. In fact, human subjects can dynamically adjust their focus and decision process based on the evaluation dimension (*e.g.*, prioritize shape and contour for geometry evaluation), resulting in diverse scores with changing perspectives. Consequently, single-dimensional evaluators may fail to capture rich quality-related factors. To comprehensively evaluate text-to-3D generation, it is essential to develop robust metrics that reflect multi-dimensional human perception.

To solve the above problems, we establish a comprehensive benchmark named **Multi-Dimensional Text-to-3D Quality Evaluation Benchmark (MATE-3D)**, which is the first contribution of this paper. MATE-3D first categorizes the prompts based on object quantity. For single object generation, we define four sub-categories based on the prompt complexity and creativity, including “*Basic*”, “*Refined*”, “*Complex*” and “*Fantastical*”. For multiple object generation, the prompts contain at least two objects with specified relationships between the objects. Based on the type of relationships, we define four sub-categories denoted by “*Grouped*”, “*Spatial*”, “*Action*”, and “*Imaginative*”. Utilizing large language models, we design 160 prompts for the eight sub-categories in total. We use these prompts as the input of eight prevalent text-to-3D methods and acquire 1,280 generated samples, which are transformed into a unified representation, *i.e.*, textured mesh. Then, we conduct

a comprehensive subjective experiment and each textured mesh is annotated by 21 human subjects from four evaluation dimensions, including *semantic alignment*, *geometry quality*, *texture quality*, and *overall quality*. A total of $1,280 \times 4 \times 21 = 107,520$ annotations are collected, and we further obtain the Mean Opinion Score (MOS) for each evaluation dimension of the generated meshes. Finally, we conduct detailed analyses of subjective scores to provide useful insight for future text-to-3D research.

Furthermore, we propose a novel quality evaluator named HyperScore for text-to-3D generation, which can perform multi-dimensional assessment by utilizing a hypernetwork to generate specified mapping function for each evaluation dimension, resulting in the second contribution. More concretely, we first use a pre-trained CLIP model to extract visual and textual features from rendered images of textured meshes and prompts. Then, we create a sequence of learnable tokens and feed them into the textual encoder to obtain multiple condition features that represent information relevant to evaluation dimensions. Using these condition features, we implement two strategies to achieve fine-grained quality evaluation across dimensions. i) We utilize the condition features to compute the fusion weights for various patches in the visual feature, which mimics the focus shift during evaluation. ii) We feed the condition features into a hypernetwork [10] to generate diverse weights of a mapping head, thereby simulating different decision-making processes aligned with changing evaluation dimensions. Experiments on MATE-3D show that HyperScore outperforms existing metrics in all evaluation dimensions. We summarize the contributions as follows:

- We establish a new benchmark, MATE-3D, for evaluating text-to-3D methods. MATE-3D contains 1,280 textured meshes generated from eight prompt categories and each sample is annotated from four evaluation dimensions.
- We propose a multi-dimensional quality evaluator, HyperScore, for text-to-3D generation. Utilizing the learnable condition features, we achieve differentiated quality predictions for multiple evaluation dimensions.
- Extensive experiments show that the proposed HyperScore presents superior performance on different evaluation dimensions than existing evaluation metrics.

2. Related Works

2.1. Text-to-3D Generation

Generating 3D objects conditioned on texts has become a challenging yet prominent research area in recent years. With the emergence of large-scale 3D datasets [3, 4], some methods, such as Point-E [40] and Shap-E [22], first train the network using 3D datasets and then generate 3D assets in a feed-forward manner [1, 8, 9, 14, 17, 67, 68]. Since the quantity of image-text pairs [25, 26] is much larger than the

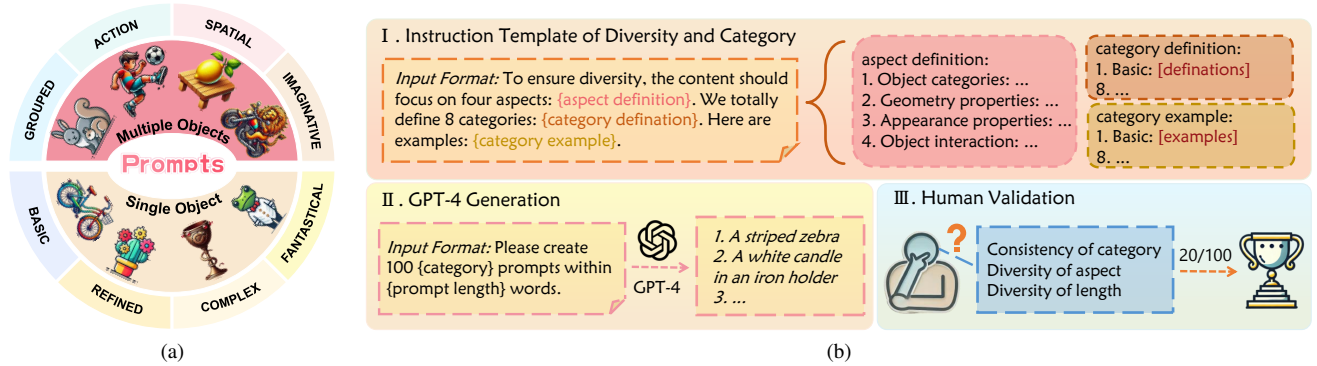


Figure 2. (a) The overview of eight prompt categories; (b) The illustration of prompt generation pipeline.

3D counterparts, Dreamfusion [42] pioneers the paradigm of optimizing 3D generation with pre-trained 2D diffusion models, which leverages Score Distillation Sampling (SDS) to optimize a NeRF. Based on this paradigm, some works [30, 36, 37, 49, 57, 71] introduce a coarse-to-fine optimization strategy with two stages and improve both speed and quality. Recent studies [21, 46, 52, 65, 66] incorporate 3DGS into generative 3D content creation, achieving acceleration compared to NeRF-based approaches. There also emerge hybrid 3D generative methods [2, 28, 34, 48, 50, 63, 64] by combining the advantage of 3D native and 2D prior-based generative methods. The typical example is One-2-3-45++ [32], which generates 3D representations by training a 3D diffusion model with the input of 2D prior-based multi-view images.

2.2. Text-to-3D Evaluation

To facilitate the text-to-3D evaluation, several benchmarks have been developed. T³Bench [12] devises three prompt suites incorporating diverse 3D scenes and with increasing complexity, including *Single object*, *Single object with surroundings*, and *Multiple objects*, and then creates 630 samples scored from two dimensions, *i.e.*, quality and alignment. Another benchmark [58] leverages GPT-4 to generate prompts with varying degrees of creativity and complexity, then evaluates preferences between 234 sample pairs generated from identical prompts across five dimensions. Overall, these benchmarks face limitations, such as insufficient prompt diversity and the absence of multi-dimensional absolute scores, emphasizing the need for a more comprehensive benchmark. Furthermore, existing evaluation metrics [14, 27, 47, 59, 62] are either limited to single-dimensional evaluations or dependent on simple pairwise comparisons, which are insufficient to face the nuanced challenges of text-to-3D generation. Consequently, there is an urgent need for a comprehensive metric capable of assessing multi-dimensional quality.

3. Benchmark Construction and Analysis

3.1. Data Preparation

Prompt Categorization. To enhance the comprehensiveness and diversity of constructed prompts, we thoroughly consider the variety of scenarios present in the real world. We first classify text prompts based on object quantity. For single object generation, we define four sub-categories including “*Basic*”, “*Refined*”, “*Complex*” and “*Fantastical*”, where the former three categories have increasing textual complexity while the last category focuses on generating object with high creativity. For multiple object generation, the text prompt is composed of at least two objects with specified relationships between the objects. Based on the type of the relationships, we define four sub-categories denoted by “*Grouped*”, “*Action*”, “*Spatial*”, and “*Imaginative*”. The *Grouped* category describes multiple objects connected by “and”; The *Action* and *Spatial* categories describe action interactions (*e.g.*, “hold”, “watch”, “play with”) and spatial (*e.g.* “on”, “near”, “on the bottom of”), respectively; “*Imaginative*” describe multiple objects with interactions, where objects or interactions should be creative. Fig. 3 shows eight exemplary prompts corresponding to different categories. We detail the definition of each category in the appendix.

Prompt Generation. Based on the defined categories, we generate well-structured prompts for each category with the assistance of GPT-4 [41] as shown in Fig. 2b. First, we follow [58] to provide an instruction to ensure that GPT-4 understands the task requirements. To promote prompt diversity, the instruction first emphasizes four aspects to consider: object categories, geometry properties, appearance properties, and object interactions. Then, the instruction defines the above eight categories with examples to ensure that the prompts generated by GPT-4 closely align with each category. Based on the instruction, we utilize GPT-4 to create a large pool of candidate prompts tailored to the identified challenges. Finally, we manually filter out any duplicate or inappropriate prompts to ensure consistency and diversity



Figure 3. Samples from the database generated by eight different generative methods.

within the benchmark. Overall, we select 20 prompts from a pool of 100 candidates for each category, resulting in a total of 160 prompts.

Mesh Generation. After the prompt generation, we adopt eight recent text-to-3D generative methods, including DreamFusion [42], Magic3D [30], Score Jacobian Chaining (SJC) [55], TextMesh [53], 3DTopia [15], Consistent3D [60], LatentNeRF [37], and One-2-3-45++ [32] to generate 3D representations by using open source code and default weight, which are then transformed into textured meshes. Finally, we obtain 1,280 textured meshes. Fig. 3 shows the mesh samples in the database along with their corresponding prompts and generative methods.

3.2. Subjective Study

Evaluation Dimension. The quality of the generated textured meshes is influenced by different factors. To provide a more nuanced understanding of human perception, we define four evaluation dimensions that need annotation:

- **Alignment.** Subjects should measure the semantic consistency of the generated meshes with the prompts, including evaluating whether the generated meshes accurately match the prompts (*e.g.*, quantity, attributes, location, relationship) and whether there is missing or redundant content.
- **Geometry.** Subjects should measure the geometry fidelity of textured meshes, including measuring the shape, contour, size, and whether there is missing or redundant structure in the generated meshes.
- **Texture.** Subjects should measure the texture details of textured meshes, including evaluating the color, material, and whether the appearance of meshes is vibrant and of

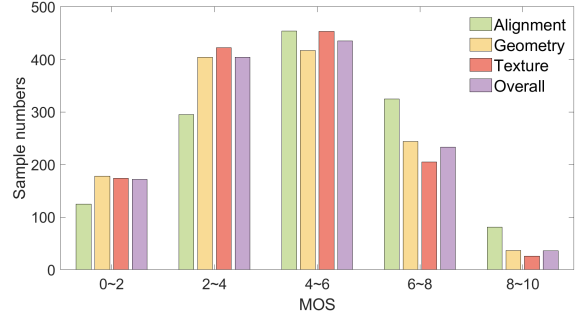


Figure 4. Distribution of MOS for four dimensions.

high resolution.

- **Overall.** Subjects should conduct a holistic assessment of the samples by integrating the insights from different perspectives.

Experiment Setup. To obtain the MOS of each mesh, we invite subjects to score the samples from the above four dimensions. We employ the 11-level impairment scale (ranging from 0 to 10) proposed by ITU-T P.910 [45] as the voting methodology. An interactive evaluation protocol is used to enable subjects to adjust their viewpoints according to their preferences. Each textured mesh is annotated by 21 human subjects from the four evaluation dimensions. After collecting the subjective scores, we implement the outlier detection method outlined in ITU-R BT.500 [44] to identify and exclude outliers from the raw data. Finally, the MOS for each dimension of one textured mesh is calculated by averaging the filtered raw scores. Fig. 4 illustrates the distribution of MOS for alignment, geometry, texture, and overall quality. We see that the benchmark covers broad quality ranges for multiple dimensions.

3.3. Observations

We conduct comprehensive analyses for the subjective scores of MATE-3D. We first investigate the relationships among different evaluation dimensions. Fig. 5a - Fig. 5c illustrate scatter plots that depict the correlations among three dimensions (*i.e.*, alignment, geometry, and texture). From Fig. 5a and Fig. 5b, we observe a relatively low correlation between the alignment and the geometry or texture score at the medium quality range (*e.g.*, [4, 6]). The reason is that the alignment evaluation mostly focuses on semantic consistency while the geometry or texture evaluation relies on specified details. For instance, in Fig. 5a, the mesh generated from the prompt “A plastic spoon and a ceramic cup” includes only a cup, resulting in a low alignment score. However, the cup itself demonstrates good geometry quality. In contrast, the sample corresponding to the prompt “A canned Coke” achieves a relatively high alignment score but suffers from an uneven surface and an incomplete shape, leading to a low geometry score. From Fig. 5c, the mutual influence between the geometry and tex-

Table 1. Average scores (in terms of overall quality) of each generative method on eight prompt categories. The values of 1-8 represent the rank in each row.

Method	Single Object				Multiple Object			
	Basic	Refined	Complex	Fantastic	Grouped	Action	Spatial	Imaginative
DreamFusion	4.99(1)	4.96(2)	4.64(4)	3.24(8)	3.45(7)	3.73(6)	4.47(3)	3.75(5)
Magic3D	5.26(1)	4.89(6)	5.06(3)	4.95(4)	3.92(8)	4.73(7)	5.06(2)	4.93(5)
SJC	3.28(2)	3.48(1)	2.95(4)	2.92(6)	2.50(8)	2.77(7)	2.92(5)	3.25(3)
TextMesh	4.08(6)	4.56(2)	4.79(1)	4.22(4)	3.22(8)	3.68(7)	4.17(5)	4.26(3)
3DTopia	5.06(1)	4.91(2)	4.83(3)	3.89(6)	4.05(4)	2.80(8)	3.89(5)	2.95(7)
Consistent3D	4.15(5)	4.92(1)	4.40(2)	4.32(4)	3.37(8)	3.64(6)	4.39(3)	3.47(7)
LatentNeRF	3.20(7)	3.76(3)	3.47(5)	4.16(1)	2.94(8)	3.48(4)	3.46(6)	4.01(2)
One-2-3-45++	7.79(1)	7.69(2)	6.50(5)	6.60(4)	6.49(6)	5.65(8)	6.81(3)	6.13(7)

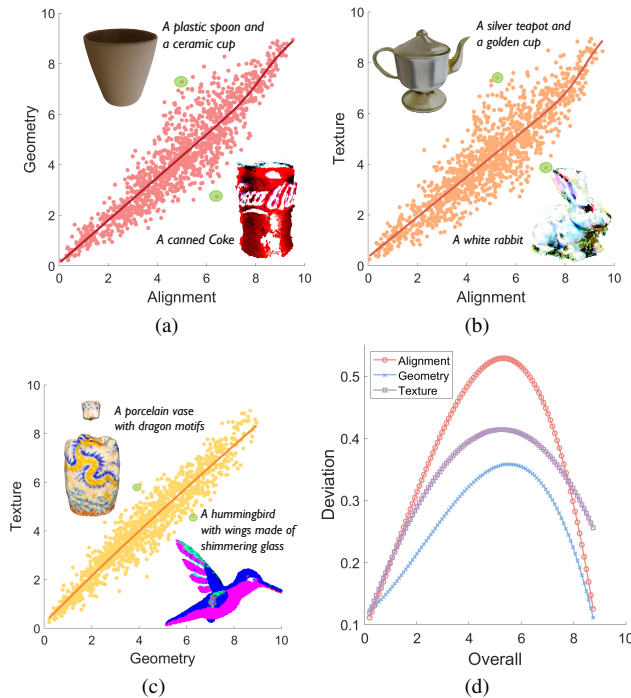


Figure 5. (a) Alignment vs. Geometry; (b) Alignment vs. Texture; (c) Geometry vs. Texture; (d) Deviations among the other three dimensions and overall quality.

ture scores is more pronounced, as the two dimensions influence each other during the generation process. Finally, in Fig. 5d, we calculate the deviations between the other three dimensions and the overall score after non-linear regression, which indicates the consistency between each dimension and the overall quality. We can see that the geometry quality is most closely related to the overall quality. It is reasonable because geometry deformations (e.g., incomplete shape, floaters) directly affect 3D perception. The alignment quality appears to have the least correlation with the overall quality because it relatively ignores some details that human subjects care about.

We further illustrate the average scores of each generative

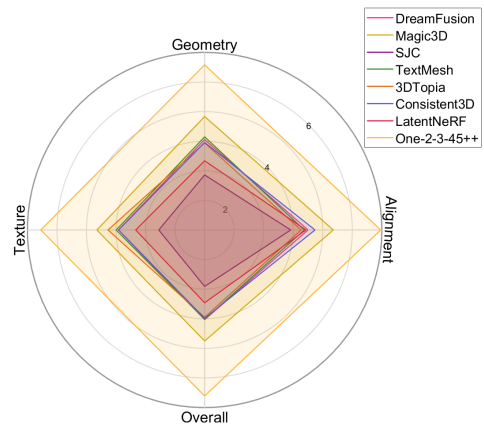


Figure 6. Average scores of different methods on the four dimensions.

ative method on the four evaluation dimensions in Fig. 6. We can see that One-2-3-45++ performs best on all dimensions, while SJC provides the worst performance. This is primarily because SJC usually causes an incomplete geometry shape and noisy floaters, making it difficult to generate high-quality samples. Other generative methods also face some difficulties during the generation process. For example, TextMesh often generates 3D objects with overly simplistic shapes, which limits their complexity and realism. 3DTopia tends to generate single object, leading to comparatively lower scores in multiple object generation. One-2-3-45++ tends to generate flatter geometric structures and blurry textures. Moreover, except for One-2-3-45++, all generative methods can cause Janus problem due to the bias of the used 2D diffusion models towards 2D front views. The bias results in repeating front views from different angles rather than generating coherent 3D objects.

To investigate the ability of the methods to generate different scenes, we report the average scores (in terms of overall quality) of each method on eight prompt categories in Tab. S8. We have the following findings: i) All methods achieve better performance for single object generation than multiple object generation. In fact, existing methods

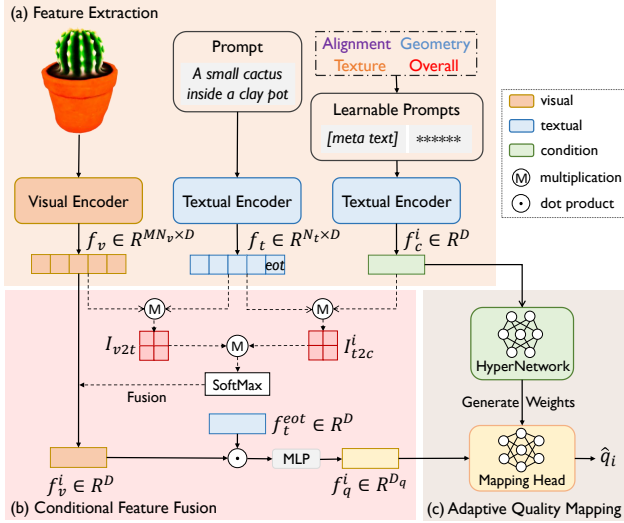


Figure 7. The framework of the proposed multi-dimensional quality evaluator.

struggle in constructing the correct relationships among objects and usually miss some contents during generation, restricting their performance in multiple object generation. ii) For the sub-categories of single object generation, the generation quality of most methods decreases with increasing prompt complexity (from *Basic* to *Refined* to *Complex*). However, there are some exceptions. For example, the generated samples of TextMesh often exhibit too simple geometric structures. Consequently, its generation for the *Basic* category may be too simplistic to discern, leading to lower scores. iii) For the sub-categories of multiple object generation, it is observed that most methods provide better performance on the *Spatial* category, followed by the *Action* and *Grouped* categories. It seems that these methods are more capable of modeling specific spatial interactions. In contrast, the *Action* prompts may introduce ambiguity with actions like “chase” or “run” because these verbs often indicate a greater distance, while the *Grouped* category usually results in overlapping or missing objects. iv) The *Fantastic* and *Imaginative* categories primarily emphasize the creativity of the prompts, allowing a wide range of object details and interactions. As a result, different methods perform inconsistently on the two categories.

4. Evaluator for Text-to-3D Generation

4.1. Problem Formulation

Given a generated mesh x and its corresponding prompt t , existing single-dimensional evaluators directly map them to the subjective score q . The procedure can be described as $\hat{q} = \psi(\phi(x, t))$, where \hat{q} is the predicted score; $\phi(\cdot)$ denotes a feature extractor such as CLIP and $\psi(\cdot)$ represents a mapping function such as the cosine similarity function in

CLIPScore [14]. Given multiple targets $\{q_i\}_{i=1}^K$ from K dimensions, a reasonable solution for multi-dimensional evaluation is a multi-task network with a shared feature extractor and multiple mapping heads, that is,

$$\hat{q}_i = \psi_i(\phi(x, t) | \theta_i), \quad (1)$$

where $\psi_i(\cdot | \theta_i)$ denotes the mapping head for the i -th dimension with the parameters θ_i . However, directly optimizing such a multi-task network may fail to exploit differentiated perception rules depending on the evaluation dimensions. Therefore, we further transform the task as follows:

$$\hat{q}_i = \psi(\phi(x, t) | \pi(f_c^i)), \quad (2)$$

where $\pi(\cdot)$ denotes a hypernetwork to generate θ_i for a unified mapping head; f_c^i denotes a condition feature related to the i -th evaluation dimension. By injecting the condition features, we can better characterize the differences among evaluation perspectives.

We illustrate the framework of our evaluator in Fig. 7, which can be divided into three stages: i) **Feature Extraction**. We first use a transformer-based CLIP model to extract visual and textual features from rendered images of textured meshes and prompts. Meanwhile, we feed a sequence of learnable prompts into the textual encoder to obtain multiple condition features corresponding to various dimensions. ii) **Conditional Feature Fusion**. We utilize the condition features to compute fusion weights for various patches in the visual features. The fused visual feature is then merged with the textual feature to obtain the final quality feature. iii) **Adaptive Quality Mapping**. We feed the condition features into a hypernetwork to generate diverse weights of the mapping head, and then regress the quality feature into the final score of the specified dimension.

4.2. Feature Extraction

For a test mesh x , we first render it into multi-view images as $\{x_r^m\}_{m=1}^M$, where M denotes the number of viewpoints. Then we resort to a pre-trained CLIP model for feature extraction, which is composed of a transformer-based visual encoder $\phi_v(\cdot)$ and a frozen textual encoder $\phi_t(\cdot)$. To better capture local distortion patterns, we use the tokens of all image patches as the output of $\phi_v(\cdot)$. The feature extraction process can be formulated as:

$$f_v^m = \phi_v(x_r^m) \in \mathbb{R}^{N_v \times D}, \quad f_t = \phi_t(t) \in \mathbb{R}^{N_t \times D}, \quad (3)$$

where N_v denotes the token number of image (*i.e.*, the patch number) and N_t denotes the token number of text. We further concatenate the visual features of different viewpoints to derive $f_v \in \mathbb{R}^{MN_v \times D}$.

Previous research [18, 69] demonstrates that specific tags (*e.g.*, “shape, edge” for geometry evaluation) can effectively

Table 2. Performance Comparison on MATE-3D. The best metric in each column is marked in **boldface**.

Metric	Alignment			Geometry			Texture			Overall		
	PLCC	SRCC	KRCC	PLCC	SRCC	KRCC	PLCC	SRCC	KRCC	PLCC	SRCC	KRCC
CLIPScore [14]	0.535	0.494	0.347	0.520	0.496	0.347	0.563	0.537	0.379	0.541	0.510	0.359
BLIPScore [27]	0.569	0.533	0.377	0.570	0.542	0.382	0.608	0.578	0.413	0.586	0.554	0.393
Aesthetic Score [47]	0.185	0.099	0.066	0.270	0.160	0.107	0.288	0.172	0.114	0.228	0.150	0.100
ImageReward [62]	0.675	0.651	0.470	0.624	0.591	0.422	0.650	0.612	0.441	0.657	0.623	0.448
HPS v2 [59]	0.477	0.416	0.290	0.455	0.412	0.286	0.469	0.423	0.296	0.465	0.420	0.293
CLIP-IQA [56]	0.151	0.039	0.025	0.223	0.125	0.084	0.264	0.163	0.108	0.213	0.115	0.076
ResNet50 + FT [11]	0.577	0.551	0.387	0.669	0.653	0.471	0.691	0.672	0.487	0.649	0.632	0.452
ViT-B + FT [6]	0.544	0.515	0.360	0.662	0.642	0.461	0.691	0.676	0.492	0.633	0.614	0.439
SwinT-B + FT [35]	0.534	0.506	0.359	0.626	0.610	0.438	0.654	0.640	0.465	0.608	0.592	0.425
MultiScore	0.657	0.638	0.458	0.719	0.703	0.516	0.746	0.729	0.540	0.714	0.698	0.511
HyperScore	0.754	0.739	0.547	0.793	0.782	0.588	0.822	0.811	0.619	0.804	0.792	0.600

capture dimension-related information. To avoid meticulous design for fixed tags, we only define K meta text about different evaluation dimensions (e.g., “alignment quality”, “geometry quality”, “texture quality”, “overall quality” for MATE-3D) and acquire the corresponding meta tokens. We further introduce the learnable prompts following CoOp [70] and insert the meta tokens in the front of a squeeze of learnable tokens to acquire K tokenized prompts as $\{t_c^i\}_{i=1}^K$. Subsequently, these tokenized prompts will pass through the frozen textual encoder to obtain a list of condition features denoted by $\{f_c^i \in \mathbb{R}^D\}_{i=1}^K$, where we only retain the EOT (end of text) token as the output because it is often used to represent the whole text.

4.3. Conditional Feature Fusion

As aforementioned, human evaluators adaptively focus on different aspects of scenes depending on the evaluation dimensions. Therefore, different patches in multiple viewpoints do not contribute equally to the final prediction; meanwhile, the contribution of each patch may change across dimensions. Based on the insight, we implement a conditional feature fusion strategy.

Specifically, we first normalize the visual, textual and condition features to obtain \tilde{f}_v , \tilde{f}_t , and $\{\tilde{f}_c^i\}_{i=1}^K$. For each evaluation dimension, we define two correlation matrices as:

$$I_{v2t} = \tilde{f}_v \cdot \tilde{f}_t^T \in \mathbb{R}^{MN_v \times N_t}, I_{t2c}^i = \tilde{f}_t \cdot (\tilde{f}_c^i)^T \in \mathbb{R}^{N_t}, \quad (4)$$

where I_{v2t} quantifies the degree of correlation between each image patch and each text token, whereas I_{t2c}^i determines the relative importance of each text token for the i -th condition. Then, we perform the conditional feature fusion for the i -th evaluation dimension as:

$$f_{v,c}^i = \text{SoftMax}(I_{v2t} \cdot I_{t2c}^i) \cdot f_v \in \mathbb{R}^D, \quad (5)$$

where $\text{SoftMax}(\cdot)$ denotes the softmax function. Based on Eq. (5), the more relevant the patch is to the condition, the

higher the weight. Finally, we derive the quality feature of the i -th dimension as:

$$f_q^i = \text{MLP}(f_{v,c}^i \odot f_t^{\text{eot}}) \in \mathbb{R}^{D_q}, \quad (6)$$

where \odot denotes the element-wise multiplication and $\text{MLP}(\cdot)$ represents a simple multi-layer perceptron; $f_t^{\text{eot}} \in \mathbb{R}^D$ indicates the EOT token in f_t .

4.4. Adaptive Quality Mapping

After obtaining the quality feature for the specified condition, we need to transform it into the corresponding quality score using a mapping function $\psi(\cdot)$ parameterized by the weights θ_i . Previous studies [51] have indicated that the mapping function can represent the decision procedure used to assess quality. We further argue that as the evaluation dimension considered varies, the decision procedure also varies. Therefore, we define $\psi(\cdot)$ as fully connected layers and use a hypernetwork $\pi(\cdot)$ to generate θ_i , i.e., $\theta_i = \pi(f_c^i)$. Two types of network parameters, i.e., fully connected layer weights and biases, are generated (please refer to the appendix for the detailed architecture of $\psi(\cdot)$ and $\pi(\cdot)$). Finally, we can infer the quality score of the i -th dimension as:

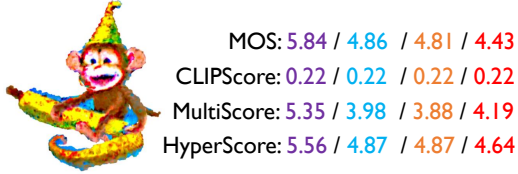
$$\hat{q}_i = \psi(f_q^i | \pi(f_c^i)). \quad (7)$$

5. Experiment

5.1. Implement Details

Training Strategy. We implement our metric by PyTorch and conduct training and testing on the NVIDIA 3090 GPUs. All textured meshes are rendered into $M = 6$ projected images with a spatial resolution of 512×512 by PyTorch3D. More details for network implementation and training such as the used loss function can be found in the appendix.

Training-test Split. We apply a 5-fold cross-validation for MATE-3D while ensuring that there is no prompt overlap between the training and testing sets. Specifically, the



MOS: 5.84 / 4.86 / 4.81 / 4.43
 CLIPScore: 0.22 / 0.22 / 0.22 / 0.22
 MultiScore: 5.35 / 3.98 / 3.88 / 4.19
 HyperScore: 5.56 / 4.87 / 4.87 / 4.64

A monkey wizard is riding a flying broom and eating a banana



MOS: 5.68 / 6.64 / 5.04 / 5.81
 CLIPScore: 0.17 / 0.17 / 0.17 / 0.17
 MultiScore: 5.89 / 5.35 / 5.13 / 5.22
 HyperScore: 5.95 / 6.61 / 5.13 / 5.97

A ceramic vase with swirling patterns etched into the surface, a chipped rim, and a long, narrow neck

Figure 8. Exemplary samples with their MOSs and the predicted scores of different metrics. The four scores in each row denote alignment, geometry, texture, and overall quality, respectively.

ratios of prompts in the training set and test set are 128:32. For each fold, the performance on the test set with minimal training loss is recorded, and the average performance across all folds is recorded as the final result.

Evaluation Metrics. We utilize Pearson Linear Correlation Coefficient (PLCC), Spearman Rank order Correlation Coefficient (SRCC), and Kendall’s Rank order Correlation Coefficient (KRCC) as performance criteria. Better metrics should have higher SRCC, KRCC, and PLCC. Before calculating PLCC, we follow [54] to map the objective score to the subject score using a logistic function.

5.2. Performance Comparison

Quantitative Analysis. Table 2 lists the experimental results on MATE-3D. We select widely used zero-shot metrics for text-to-image(or 3D) evaluation, including CLIPScore [14], BLIPScore [27], Aesthetic Score [47], ImageReward [62], HPS v2 [59], and CLIP-IQA [56]. Note that we average the scores of multiple rendered viewpoints for these metrics. In addition, we also equip some prevalent backbones (including ResNet50 [11], ViT-B [6], SwinT-B [35]) pre-trained on ImageNet [5] with multiple regression heads and fine-tune them on MATE-3D. Finally, we propose a baseline named MultiScore that has the same feature extractor as HyperScore but only applies a multi-task learning strategy. All results are averaged after 5-fold splitting.

From Tab. 2, we have the following observations: i) The proposed HyperScore exhibits outstanding performance across all evaluation dimensions, which demonstrates its effectiveness for multi-dimensional assessment. Especially,

Table 3. Ablation study for the key modules. ‘✓’ or ‘✗’ means the setting is preserved or discarded.

Index	CFF	AQM	Alignment	Geometry	Texture	Overall
(1)	✗	✗	0.638	0.703	0.729	0.698
(2)	✓	✗	0.660	0.730	0.760	0.724
(3)	✗	✓	0.721	0.762	0.792	0.776
(4)	✓	✓	0.739	0.782	0.811	0.792

HyperScore presents a noticeable gain over MultiScore, justifying the potential of conditional learning strategy. ii) ImageReward performs best among these zero-shot metrics, which may be attributed to its rank-based training strategy. iii) Aesthetic Score provides inferior results, probably due to its preference for aesthetic quality. CLIP-IQA also performs poorly, possibly because they are designed for natural images instead of rendered images of textured meshes.

Qualitative Analysis. For better illustration, we also conduct a qualitative analysis on several examples shown in Fig. 8. From the figure, we can see: i) One sample has diverse scores for different quality dimensions, highlighting the drawbacks of traditional evaluators (e.g., CLIPScore) because they can only provide a single score. ii) MultiScore gives similar scores for different dimensions, which affects the judgment for different factors. For the first sample, MultiScore gives a lower score for texture quality than for overall quality (3.88 vs. 4.19), which contradicts the subjective rating (4.81 vs. 4.43). In contrast, HyperScore achieves a more discriminated prediction and presents an accurate ranking between the above two dimensions (4.87 vs. 4.64), further demonstrating the effectiveness of our metric.

5.3. Ablation Study

To verify the effectiveness of the key modules, we further investigate the contribution of different components and report the results (in terms of SRCC) in Tab. 3. In the table, CFF and AQM denote conditional feature fusion and adaptive quality mapping, respectively. The baseline (denoted by (1)) applies a multi-task learning strategy and simply averages all patches in the visual feature. From the table, we can see: i) Comparing (2) or (3) with (1), both CFF and AQM contribute to the metric performance, demonstrating the effectiveness of the two modules. Especially, the AQM brings noticeable gain over the baseline, justifying the use of hypernetwork in our metric. ii) Seeing (2)-(4), the full model performs better than using only single module, which verifies the complementarity of the two modules. More ablation studies can be found in the appendix.

6. Conclusion

In this paper, we are dedicated to exploring a subjective-aligned quality evaluation for text-to-3D generation. For this purpose, we first establish a comprehensive benchmark

named MATE-3D. The benchmark contains eight prompt categories and 1,280 textured mesh samples annotated from four evaluation dimensions. Based on MATE-3D, we propose a multi-dimensional quality evaluator named HyperScore. Based on the merits of hypernetwork, the evaluator can perform adaptive prediction according to changing evaluation perspectives. Experimental results indicate that HyperScore is effective in evaluating text-to-3D generation.

References

- [1] Anpei Chen, Haofei Xu, Stefano Esposito, Siyu Tang, and Andreas Geiger. Lara: Efficient large-baseline radiance fields. In *European Conference on Computer Vision (ECCV)*, 2025. 2
- [2] Cheng Chen, Xiaofeng Yang, Fan Yang, Chengzeng Feng, Zhoujie Fu, Chuan-Sheng Foo, Guosheng Lin, and Fayao Liu. Sculpt3d: Multi-view consistent text-to-3d generation with sparse 3d prior. In *IEEE/CVF Conference on Computer Vision and Pattern Recognition (CVPR)*, 2024. 3
- [3] Matt Deitke, Ruoshi Liu, Matthew Wallingford, Huong Ngo, Oscar Michel, Aditya Kusupati, Alan Fan, Christian Laforte, Vikram Voleti, Samir Yitzhak Gadre, Eli VanderBilt, Anirudha Kembhavi, Carl Vondrick, Georgia Gkioxari, Kiana Ehsani, Ludwig Schmidt, and Ali Farhadi. Objaverse-xl: A universe of 10m+ 3d objects. In *Advances in Neural Information Processing Systems (NIPS)*, 2023. 2
- [4] Matt Deitke, Dustin Schwenk, Jordi Salvador, Luca Weihs, Oscar Michel, Eli VanderBilt, Ludwig Schmidt, Kiana Ehsani, Anirudha Kembhavi, and Ali Farhadi. Objaverse: A universe of annotated 3d objects. In *IEEE/CVF Conference on Computer Vision and Pattern Recognition (CVPR)*, 2023. 2
- [5] Jia Deng, Wei Dong, Richard Socher, Li-Jia Li, Kai Li, and Li Fei-Fei. Imagenet: A large-scale hierarchical image database. In *IEEE/CVF Conference on Computer Vision and Pattern Recognition (CVPR)*, 2009. 8
- [6] Alexey Dosovitskiy. An image is worth 16x16 words: Transformers for image recognition at scale. *arXiv preprint arXiv:2010.11929*, 2020. 7, 8, 15
- [7] Ruigang Fu, Qingyong Hu, Xiaohu Dong, Yulan Guo, Yinghui Gao, and Biao Li. Axiom-based grad-cam: Towards accurate visualization and explanation of cnns. *arXiv preprint arXiv:2008.02312*, 2020. 16
- [8] Rao Fu, Xiao Zhan, Yiwen Chen, Daniel Ritchie, and Srinath Sridhar. Shapecrafter: A recursive text-conditioned 3d shape generation model. In *Advances in Neural Information Processing Systems (NIPS)*, 2022. 2
- [9] Jun Gao, Tianchang Shen, Zian Wang, Wenzheng Chen, Kangxue Yin, Daiqing Li, Or Litany, Zan Gojcic, and Sanja Fidler. Get3d: A generative model of high quality 3d textured shapes learned from images. In *Advances in Neural Information Processing Systems (NIPS)*, 2022. 2
- [10] David Ha, Andrew M Dai, and Quoc V Le. Hypernetworks. In *International Conference on Learning Representations (ICLR)*, 2022. 2
- [11] Kaiming He, Xiangyu Zhang, Shaoqing Ren, and Jian Sun. Deep residual learning for image recognition. In *IEEE/CVF Conference on Computer Vision and Pattern Recognition (CVPR)*, 2016. 7, 8
- [12] Yuze He, Yushi Bai, Matthieu Lin, Wang Zhao, Yubin Hu, Jenny Sheng, Ran Yi, Juanzi Li, and Yong-Jin Liu. T³bench: Benchmarking current progress in text-to-3d generation. *arXiv preprint arXiv:2310.02977*, 2023. 1, 2, 3, 14
- [13] Yuze He, Peng Wang, Yubin Hu, Wang Zhao, Ran Yi, Yong-Jin Liu, and Wenping Wang. Mmpi: a flexible radiance field representation by multiple multi-plane images blending. In *International Conference on Robotics and Automation (ICRA)*, 2024. 1
- [14] Jack Hessel, Ari Holtzman, Maxwell Forbes, Ronan Le Bras, and Yejin Choi. CLIPScore: A reference-free evaluation metric for image captioning. In *Empirical Methods in Natural Language Processing (EMNLP)*, 2021. 2, 3, 6, 7, 8
- [15] Fangzhou Hong, Jiayang Tang, Ziang Cao, Min Shi, Tong Wu, Zhaoxi Chen, Tengfei Wang, Liang Pan, Dahua Lin, and Ziwei Liu. 3dtopia: Large text-to-3d generation model with hybrid diffusion priors. *arXiv preprint arXiv:2403.02234*, 2024. 4, 13
- [16] Susung Hong, Donghoon Ahn, and Seungryong Kim. Debiasing scores and prompts of 2d diffusion for view-consistent text-to-3d generation. In *Advances in Neural Information Processing Systems (NIPS)*, 2023. 1
- [17] Yicong Hong, Kai Zhang, Jiuxiang Gu, Sai Bi, Yang Zhou, Difan Liu, Feng Liu, Kalyan Sunkavalli, Trung Bui, and Hao Tan. Lrm: Large reconstruction model for single image to 3d. In *International Conference on Learning Representations (ICLR)*, 2024. 2
- [18] Jingwen Hou, Weisi Lin, Yuming Fang, Haoning Wu, Chaofeng Chen, Liang Liao, and Weide Liu. Towards transparent deep image aesthetics assessment with tag-based content descriptors. *IEEE Transactions on Image Processing (TIP)*, 2023. 6
- [19] Yi-Hua Huang, Yan-Pei Cao, Yu-Kun Lai, Ying Shan, and Lin Gao. Nerf-texture: Texture synthesis with neural radiance fields. In *ACM SIGGRAPH*, 2023. 1
- [20] Ka-Hei Hui, Aditya Sanghi, Arianna Rampini, Kamal Rahimi Malekshan, Zhengzhe Liu, Hooman Shayani, and Chi-Wing Fu. Make-a-shape: a ten-million-scale 3D shape model. In *International Conference on Machine Learning (ICML)*, 2024. 2
- [21] Vishnu Jaganathan, Hannah Hanyun Huang, Muhammad Zubair Irshad, Varun Jampani, Amit Raj, and Zsolt Kira. Ice-g: Image conditional editing of 3d gaussian splats. *arXiv preprint arXiv:2406.08488*, 2024. 3
- [22] Heewoo Jun and Alex Nichol. Shap-e: Generating conditional 3d implicit functions. *arXiv preprint arXiv:2305.02463*, 2023. 2
- [23] Bernhard Kerbl, Georgios Kopanas, Thomas Leimkühler, and George Drettakis. 3d gaussian splatting for real-time radiance field rendering. *ACM Transactions On Graphics (TOG)*, 2023. 1
- [24] Diederik P Kingma and Jimmy Ba. Adam: A method for stochastic optimization. *arXiv preprint arXiv:1412.6980*, 2014. 16

- [25] Chunyi Li, Tengchuan Kou, Yixuan Gao, Yuqin Cao, Wei Sun, Zicheng Zhang, Yingjie Zhou, Zhichao Zhang, Weixia Zhang, Haoning Wu, Xiaohong Liu, Xiongkuo Min, and Guangtao Zhai. Aigiq-20k: A large database for ai-generated image quality assessment. In *IEEE/CVF Conference on Computer Vision and Pattern Recognition Workshops (CVPRW)*, 2024. 2
- [26] Chunyi Li, Zicheng Zhang, Haoning Wu, Wei Sun, Xiongkuo Min, Xiaohong Liu, Guangtao Zhai, and Weisi Lin. Aigiq-3k: An open database for ai-generated image quality assessment. *IEEE Transactions on Circuits and Systems for Video Technology (TCSVT)*, 2024. 2
- [27] Junnan Li, Dongxu Li, Caiming Xiong, and Steven Hoi. Blip: Bootstrapping language-image pre-training for unified vision-language understanding and generation. In *International Conference on Machine Learning (ICML)*, 2022. 2, 3, 7, 8
- [28] Ming Li, Pan Zhou, Jia-Wei Liu, Jussi Keppo, Min Lin, Shuicheng Yan, and Xiangyu Xu. Instant3d: Instant text-to-3d generation. *International Journal of Computer Vision (IJCV)*, 2024. 3
- [29] Three.js Library. <https://threejs.org>. 14
- [30] Chen-Hsuan Lin, Jun Gao, Luming Tang, Towaki Takikawa, Xiaohui Zeng, Xun Huang, Karsten Kreis, Sanja Fidler, Ming-Yu Liu, and Tsung-Yi Lin. Magic3d: High-resolution text-to-3d content creation. In *IEEE/CVF Conference on Computer Vision and Pattern Recognition (CVPR)*, 2023. 3, 4, 13
- [31] Jian Liu, Xiaoshui Huang, Tianyu Huang, Lu Chen, Yuenan Hou, Shixiang Tang, Ziwei Liu, Wanli Ouyang, Wangmeng Zuo, Junjun Jiang, et al. A comprehensive survey on 3d content generation. *arXiv preprint arXiv:2402.01166*, 2024. 1
- [32] Minghua Liu, Ruoxi Shi, Linghao Chen, Zhuoyang Zhang, Chao Xu, Xinyue Wei, Hansheng Chen, Chong Zeng, Jiayuan Gu, and Hao Su. One-2-3-45++: Fast single image to 3d objects with consistent multi-view generation and 3d diffusion. In *IEEE/CVF Conference on Computer Vision and Pattern Recognition (CVPR)*, 2024. 3, 4, 13
- [33] Ruoshi Liu, Rundi Wu, Basile Van Hoorick, Pavel Tokmakov, Sergey Zakharov, and Carl Vondrick. Zero-1-to-3: Zero-shot one image to 3d object. In *International Conference on Computer Vision (ICCV)*, 2023. 13
- [34] Yibo Liu, Zheyuan Yang, Guile Wu, Yuan Ren, Kejian Lin, Bingbing Liu, Yang Liu, and Jinjun Shan. Vqa-diff: Exploiting vqa and diffusion for zero-shot image-to-3d vehicle asset generation in autonomous driving. In *European Conference on Computer Vision (ECCV)*, 2024. 3
- [35] Ze Liu, Yutong Lin, Yue Cao, Han Hu, Yixuan Wei, Zheng Zhang, Stephen Lin, and Baining Guo. Swin transformer: Hierarchical vision transformer using shifted windows. In *IEEE/CVF Conference on Computer Vision and Pattern Recognition (CVPR)*, 2021. 7, 8
- [36] Zhiyuan Ma, Yuxiang Wei, Yabin Zhang, Xiangyu Zhu, Zhen Lei, and Lei Zhang. Scaledreamer: Scalable text-to-3d synthesis with asynchronous score distillation. In *European Conference on Computer Vision (ECCV)*, 2024. 3
- [37] Gal Metzer, Elad Richardson, Or Patashnik, Raja Giryes, and Daniel Cohen-Or. Latent-nerf for shape-guided generation of 3d shapes and textures. In *IEEE/CVF Conference on Computer Vision and Pattern Recognition (CVPR)*, 2023. 3, 4, 13
- [38] Ben Mildenhall, Pratul P Srinivasan, Matthew Tancik, Jonathan T Barron, Ravi Ramamoorthi, and Ren Ng. Nerf: Representing scenes as neural radiance fields for view synthesis. In *European Conference on Computer Vision (ECCV)*, 2020. 1
- [39] Nasir Mohammad Khalid, Tianhao Xie, Eugene Belilovsky, and Tiberiu Popa. Clip-mesh: Generating textured meshes from text using pretrained image-text models. In *ACM SIGGRAPH Asia*, 2022. 2
- [40] Alex Nichol, Heewoo Jun, Prfulla Dhariwal, Pamela Mishkin, and Mark Chen. Point-e: A system for generating 3d point clouds from complex prompts. *arXiv preprint arXiv:2212.08751*, 2022. 2
- [41] OpenAI. Gpt-4 system card. *OpenAI*, 2023. 3, 12
- [42] Ben Poole, Ajay Jain, Jonathan T. Barron, and Ben Mildenhall. Dreamfusion: Text-to-3d using 2d diffusion. In *International Conference on Learning Representations (ICLR)*, 2023. 1, 3, 4, 13
- [43] Alec Radford, Jong Wook Kim, Chris Hallacy, Aditya Ramesh, Gabriel Goh, Sandhini Agarwal, Girish Sastry, Amanda Askell, Pamela Mishkin, Jack Clark, et al. Learning transferable visual models from natural language supervision. In *International Conference on Machine Learning (ICML)*, 2021. 2
- [44] ITU-R BT.500 Recommendation. Methodologies for the subjective assessment of the quality of television images. 2019. 4, 14
- [45] ITU-T P.910 Recommendation. Subjective video quality assessment methods for multimedia applications. 1999. 4
- [46] Jiawei Ren, Liang Pan, Jiayang Tang, Chi Zhang, Ang Cao, Gang Zeng, and Ziwei Liu. Dreamgaussian4d: Generative 4d gaussian splatting. *arXiv preprint arXiv:2312.17142*, 2023. 1, 3
- [47] Christoph Schuhmann, Romain Beaumont, Richard Vencu, Cade Gordon, Ross Wightman, Mehdi Cherti, Theo Coombes, Aarush Katta, Clayton Mullis, Mitchell Wortsman, et al. Laion-5b: An open large-scale dataset for training next generation image-text models. In *Advances in Neural Information Processing Systems (NIPS)*, 2022. 2, 3, 7, 8
- [48] Junyoung Seo, Susung Hong, Wooseok Jang, Inès Hyeonsu Kim, Min-Seop Kwak, Doyup Lee, and Seungryong Kim. Retrieval-augmented score distillation for text-to-3d generation. In *International Conference on Machine Learning (ICML)*, 2024. 3
- [49] Junyoung Seo, Wooseok Jang, Min-Seop Kwak, Hyeonsu Kim, Jaehoon Ko, Junho Kim, Jin-Hwa Kim, Jiyoun Lee, and Seungryong Kim. Let 2d diffusion model know 3d-consistency for robust text-to-3d generation. In *International Conference on Learning Representations (ICLR)*, 2024. 3
- [50] Yichun Shi, Peng Wang, Jianglong Ye, Mai Long, Kejie Li, and Xiao Yang. Mvdream: Multi-view diffusion for 3d generation. *arXiv preprint arXiv:2308.16512*, 2024. 3
- [51] Shaolin Su, Qingsen Yan, Yu Zhu, Cheng Zhang, Xin Ge, Jinqiu Sun, and Yanning Zhang. Blindly assess image quality in the wild guided by a self-adaptive hyper network.

- In *IEEE/CVF Conference on Computer Vision and Pattern Recognition (CVPR)*, 2020. 7
- [52] Jiaxiang Tang, Jiawei Ren, Hang Zhou, Ziwei Liu, and Gang Zeng. Dreamgaussian: Generative gaussian splatting for efficient 3d content creation. In *International Conference on Learning Representations (ICLR)*, 2024. 1, 3
- [53] Christina Tsalicoglou, Fabian Manhardt, Alessio Tonioni, Michael Niemeyer, and Federico Tombari. Textmesh: Generation of realistic 3d meshes from text prompts. In *International Conference on 3D Vision (3DV)*, 2024. 1, 2, 4, 13
- [54] VQEG. Final report from the video quality experts group on the validation of objective models of video quality assessment. In [online], 2020. 8
- [55] Haochen Wang, Xiaodan Du, Jiahao Li, Raymond A. Yeh, and Gregory Shakhnarovich. Score jacobian chaining: Lifting pretrained 2d diffusion models for 3d generation. In *IEEE/CVF Conference on Computer Vision and Pattern Recognition (CVPR)*, 2023. 4, 13
- [56] Jianyi Wang, Kelvin CK Chan, and Chen Change Loy. Exploring clip for assessing the look and feel of images. In *AAAI Conference on Artificial Intelligence*, 2023. 7, 8
- [57] Zhengyi Wang, Cheng Lu, Yikai Wang, Fan Bao, Chongxuan Li, Hang Su, and Jun Zhu. Prolificdreamer: high-fidelity and diverse text-to-3d generation with variational score distillation. In *Advances in Neural Information Processing Systems (NIPS)*, 2024. 2, 3
- [58] Tong Wu, Guandao Yang, Zhibing Li, Kai Zhang, Ziwei Liu, Leonidas Guibas, Dahua Lin, and Gordon Wetzstein. Gpt-4v(ision) is a human-aligned evaluator for text-to-3d generation. In *IEEE/CVF Conference on Computer Vision and Pattern Recognition (CVPR)*, 2024. 2, 3, 14
- [59] Xiaoshi Wu, Yiming Hao, Keqiang Sun, Yixiong Chen, Feng Zhu, Rui Zhao, and Hongsheng Li. Human preference score v2: A solid benchmark for evaluating human preferences of text-to-image synthesis. *arXiv preprint arXiv:2306.09341*, 2023. 2, 3, 7, 8
- [60] Zike Wu, Pan Zhou, Xuanyu Yi, Xiaoding Yuan, and Hanwang Zhang. Consistent3d: Towards consistent high-fidelity text-to-3d generation with deterministic sampling prior. In *IEEE/CVF Conference on Computer Vision and Pattern Recognition (CVPR)*, 2024. 4, 13
- [61] Jiale Xu, Xintao Wang, Weihao Cheng, Yan-Pei Cao, Ying Shan, Xiaohu Qie, and Shenghua Gao. Dream3d: Zero-shot text-to-3d synthesis using 3d shape prior and text-to-image diffusion models. In *IEEE/CVF Conference on Computer Vision and Pattern Recognition (CVPR)*, 2023. 2
- [62] Jiazheng Xu, Xiao Liu, Yuchen Wu, Yuxuan Tong, Qinkai Li, Ming Ding, Jie Tang, and Yuxiao Dong. Imagereward: Learning and evaluating human preferences for text-to-image generation. In *Advances in Neural Information Processing Systems (NIPS)*, 2024. 2, 3, 7, 8
- [63] Xianghui Yang, Yan Zuo, Sameera Ramasinghe, Loris Bazzani, Gil Avraham, and Anton van den Hengel. Viewfusion: Towards multi-view consistency via interpolated denoising. In *IEEE/CVF Conference on Computer Vision and Pattern Recognition (CVPR)*, 2024. 3
- [64] Jiangleong Ye, Peng Wang, Kejie Li, Yichun Shi, and Heng Wang. Consistent-1-to-3: Consistent image to 3d view synthesis via geometry-aware diffusion models. In *International Conference on 3D Vision (3DV)*, 2024. 3
- [65] Taoran Yi, Jiemin Fang, Junjie Wang, Guanjun Wu, Lingxi Xie, Xiaopeng Zhang, Wenyu Liu, Qi Tian, and Xinggang Wang. Gaussiandreamer: Fast generation from text to 3d gaussians by bridging 2d and 3d diffusion models. In *IEEE/CVF Conference on Computer Vision and Pattern Recognition (CVPR)*, 2024. 1, 3
- [66] Taoran Yi, Jiemin Fang, Zanwei Zhou, Junjie Wang, Guanjun Wu, Lingxi Xie, Xiaopeng Zhang, Wenyu Liu, Xinggang Wang, and Qi Tian. Gaussiandreamerpro: Text to manipulable 3d gaussians with highly enhanced quality. *arXiv preprint arXiv:2406.18462*, 2024. 3
- [67] Biao Zhang, Jiapeng Tang, Matthias Nießner, and Peter Wonka. 3dshape2vecset: A 3d shape representation for neural fields and generative diffusion models. *ACM Transactions On Graphics (TOG)*, 2023. 2
- [68] Longwen Zhang, Ziyu Wang, Qixuan Zhang, Qiwei Qiu, Anqi Pang, Haoran Jiang, Wei Yang, Lan Xu, and Jingyi Yu. Clay: A controllable large-scale generative model for creating high-quality 3d assets. *ACM Transactions on Graphics (TOG)*, 2024. 2
- [69] Sixian Zhang, Bohan Wang, Junqiang Wu, Yan Li, Tingting Gao, Di Zhang, and Zhongyuan Wang. Learning multi-dimensional human preference for text-to-image generation. In *IEEE/CVF Conference on Computer Vision and Pattern Recognition (CVPR)*, 2024. 6
- [70] Kaiyang Zhou, Jingkang Yang, Chen Change Loy, and Ziwei Liu. Learning to prompt for vision-language models. *International Journal of Computer Vision (IJCV)*, 2022. 7
- [71] Junzhe Zhu, Peiye Zhuang, and Sanmi Koyejo. Hifa: High-fidelity text-to-3d generation with advanced diffusion guidance. In *International Conference on Learning Representations (ICLR)*, 2024. 3

Appendix

A. Overview

This appendix includes additional details on benchmark construction, evaluator implementation, and experiment results, which cannot be fully covered in the main paper due to limited space. In Appendix B, we first introduce more details about the benchmark construction, including the definition of eight prompt categories and the instruction used in GPT-4. Then, we present more implementation details about the proposed evaluator, including network details and training strategy in Appendix C. Finally, we provide additional experimental results to demonstrate the effectiveness of our metric in Appendix D.

B. More Details on Benchmark Construction

B.1. Definition of Different Prompt Categories

Considering the number of objects and their complexity, creativity, and relationship, we define eight prompt categories in our benchmark. The definitions of these categories are reported as follows:

- *Basic*. Descriptions about a single object without detailed geometry or appearance details, where some global properties (e.g., color, shape, material) could be included. Examples: “A green apple”, “A square table”, and “A wooden chair”.
- *Refined*. Descriptions about a single object with one simple specification of the geometry or appearance details. Examples: “A yellow rubber duck has only one foot”, “A plastic cup with a printed logo”, and “An imperial state crown of England”.
- *Complex*. Descriptions about a single object with more than two detailed specifications of geometry or appearance details. Examples: “A brown teddy bear, fur matted, one eye missing”, “A turtle standing on its hind legs, wearing a top hat and holding a cane”, and “An oversized, porous, sphere-shaped birdcage, made of woven golden wires”.
- *Fantastical*. Descriptions about a single object with high creativities that are not, or are generally unlikely to be, found in the real world. Examples: “A frog with a translucent skin displaying a mechanical heart beating”, “A white cat has three tails, made of white, purple and black crystals”, and “A tiger dressed as a doctor”.
- *Grouped*. Descriptions about multiple objects without interactions, where some global properties (e.g., color, shape, material) could be included. Examples: “A delicious hamburger and a green apple”, “A red pig and a huge drum”, and “A round table and a square chair”.
- *Action*. Descriptions about multiple objects with interaction about action relations, where some geometry or appearance details could be included. Examples: “A hu-

manoid robot with a top hat is playing the cello”, “A black cat with white feet is sleeping peacefully beside a carved pumpkin”, and “A dog is eating a red apple with its tail raised”.

- *Spatial*. Descriptions about multiple objects with interactions about spatial relations, where some geometry or appearance details could be included. Examples: “A red apple on a round ceramic plate”, “A strong football player wearing a number seven jersey next to a blue soccer”, and “A blue rose in a crystal, symmetrical vase”.
- *Imaginative*. Descriptions about multiple objects with interactions, where objects or interactions are not or are generally unlikely to be found in the real world. Examples: “A panda with a wizard hat is reading a newspaper”, “A ghost is eating a golden apple”, and “A raccoon astronaut is holding his helmet”.

B.2. Prompt Generation

To ensure the comprehensiveness and diversity of prompts generated by GPT-4 [41], we define four aspects to consider during the prompt generation: object categories, geometry properties, appearance properties, and object interactions. These aspects are detailed as follows:

- **Object Categories**. To ensure that the generated prompts encompass the most common object classes relevant to text-to-3D tasks, we first establish clear definitions for object categories, such as “live beings”, “animals”, “plants” and so on. This approach ensures prompt diversity and avoids the generated prompts being limited to a single category.
- **Geometry Properties**. To generate more vivid and realistic 3D objects, it is essential to include detailed descriptions of geometry properties in prompts. Objects can be characterized based on their volume, shape, or size, including terms such as “symmetrical”, “cylinder”, and “small”.
- **Appearance Properties**. Similar to geometry properties, appearance properties are essential for prompt generation. Common attributes include colors, which are frequently used to describe objects’ appearance, and textures, which capture surface characteristics such as “smooth”, “rough”, and “furry”. Additionally, materials, such as “metal”, “glass”, and “fabric”, also play a significant role in defining appearance.
- **Object Interactions**. Object interactions can be classified into two types: spatial and action relationships. Spatial relationships utilize terms such as “on” and “below” to accurately define the positional relationships between objects. Action relationships describe the actions or behaviors of objects, including verbs like “wear”, “watch”, and “hold”. By integrating these words with different object categories, GPT-4 can generate prompts encompassing various interactions.



Figure S1. Training samples used in our subjective experiment.

After defining eight prompt categories and four aspects, we design a universal template to provide GPT-4 with essential context for the prompt generation task. Detailed instructions are shown in Fig. S8 and Fig. S9. Following these instructions, GPT-4 can gain a foundational understanding of the task and generate a list of prompts based on evaluator input. By editing prompt categories and lengths, GPT-4 can efficiently produce prompts across different categories.

B.3. Mesh Generation and Visualization

In recent years, significant advancements have been made in 3D generative methods. In this paper, we employ DreamFusion [42], Magic3D [30], SJC [55], TextMesh [53], 3DTopia [15], Consistent3D [60], LatentNeRF [37], and One-2-3-45++ [32] to generate 3D textured meshes. Here, we provide a brief introduction of each method.

- **DreamFusion** pioneers the paradigm of optimizing a unique 3D representation per text input or image, guided by powerful pre-trained 2D diffusion models.
- **Magic3D** introduces a coarse-to-fine optimization strategy with two stages. This approach improves both speed and quality.
- **SJC** converts a pre-trained 2D diffusion generative model on images into a 3D generative model of radiance fields, without requiring access to any 3D data.
- **TextMesh** employs a novel way to fine-tune the mesh texture, removing the effect of high saturation and improving



Figure S2. Illustration of the environment platform.

the details of the output textured mesh.

- **3DTopia** is a two-stage text-to-3D generation method. The first stage uses a diffusion model to quickly generate candidates. The second stage refines the assets chosen from the first stage. It can generate high-quality general 3D assets within 5 minutes using hybrid diffusion priors.
- **Consistent3D** uses deterministic sampling priority to ensure that different generated results are visually more consistent and have higher details when generating 3D objects. Compared to traditional random sampling methods, this approach reduces variability in generated results, ensuring that the produced 3D objects align more consistently with the specified text prompt.
- **LatentNeRF** guides the 3D generation process by encoding shape information in latent space. In this way, it can more effectively generate high-quality textures and shapes that match specific shapes while preserving details.
- **One-2-3-45++** advances multi-view 3D generation via an enhanced Zero123 [33] module enabling simultaneous cross-view attention, alongside a multi-view conditioned 3D diffusion module performing coarse-to-fine textured mesh prediction over time.

We present additional generated samples along with the evaluation scores for each method in Fig. S10.

B.4. Subjective Experiment Procedure

Training Session. Before the subjective experiment, we scale the generated meshes proportionally to ensure that each mesh fits within a cube defined by the range $[-1, 1]$. To enhance the reliability of the subjective scores, we use 10 samples whose corresponding prompts are excluded from MATE-3D to train subjects, helping them understand the rating rules. The training samples are selected to represent a comprehensive quality range, allowing viewers to understand the dataset comprehensively. We assign reference scores to the training samples and present the samples twice, requiring viewers to score them during the second viewing. If the scores given by the viewers show a high correlation with the reference scores, we conclude that they

Table S1. Comparison of the existing text-to-3D datasets. ‘✗’ represents the scores are not available.

Benchmark	Prompt Categories	Number of Generative Methods	Rating Dimensions	Number of Annotated Samples	Number of Rating Score	Annotation Type
T ³ Bench [12]	Single Object, Single Object with Surroundings, Multiple Objects	7	Alignment, Quality	630	630 × 2 × unknown	✗ (Absolute Score)
GPTEval3D [58]	Creativity, Complexity	13	Text-Asset Alignment, 3D Plausibility, Texture details, Geometry details, Texture-geometry coherency	234 pairs	234 × 5 × 3	✗ (Preference Score)
MATE-3D	Basic, Refined, Complex, Fantastical, Grouped, Action, Spatial, Imaginative	8	Alignment, Geometry, Texture, Overall	1,280	1,280 × 4 × 21	✓ (Absolute Score)

have grasped the rating principles and can provide reliable scores. Conversely, if viewers assign biased scores from the references, we repeat the training procedure until they provide reasonable results. The 10 training samples are illustrated in Fig. S1.

Experimental Environment. To enable subjects to observe 3D objects from various viewpoints and provide more accurate ratings, we employ an interactive approach for the experiment. Our interactive renderer is developed as a web application utilizing the Three.js library [29]. To effectively capture the scene, we employ an orthographic camera, with its field of view defined by the camera frustum. Subjects can control the camera’s orientation through mouse movements, which enables them to adjust their viewpoints dynamically. To minimize the influence of the background on the subjects’ evaluation, we set the background color to gray, specifically implemented using the code `scene.background = newTHREE.Color(0xaaaaaa)`. The platform, as illustrated in Fig. S2, allows subjects to navigate between previous and next samples and rate scores from four dimensions. The subjective experiment is conducted on 27-inch AOC Q2790PQ monitors with a resolution of 2560×1440 in an indoor laboratory environment under standard lighting conditions.

Outlier Detection. In total, we generate 1,280 textured meshes from 160 prompts with eight generative methods. To mitigate visual fatigue associated with prolonged experiment durations, we randomly divide the 1,280 samples into 10 sessions. To detect outliers during the subjective experiment, each rating session includes one extremely low-quality sample and one duplicate sample as “trapping samples”. Consequently, each session comprises 130 samples. After collecting the subjective scores, we implement two consecutive steps to identify outliers from the raw data. First, we identify outliers based on the “trapping samples” results. If a subject provides a high score that exceeds the expected threshold for the extremely low-quality sample or provides significantly different scores for the two duplicate samples, we exclude the raw scores of the subject from our

analysis. Second, we apply the outlier detection method described in ITU-R BT.500 [44] to conduct a further examination, removing any additional outliers identified through this process. As a result, four outliers are identified and eliminated from the subjective scores. Finally, we collect 17 scores for each sample.

B.5. Comparison with Other Benchmarks

Previous works [12, 58] have presented some text-to-3D benchmarks. We compare MATE-3D with the existing benchmarks from multiple perspectives in Tab. S1. Note that for the column of “Number of Annotated Samples”, T³Bench and MATE-3D provide “Absolute Score” for each sample, whereas GPTEval3D creates pairs of two samples and assigns ranking orders, referred to as “Preference Score” within each pair. The column of “Number of Rating Scores” is calculated as “Number of Annotated Samples” × “Number of Rating Dimensions” × “Subject Number for Each Sample”. Additionally, since the scores for T³Bench and GPTEval3D are not publicly available, we cannot evaluate the performance of objective metrics on these two benchmarks.

From Tab. S1, it is clear that our benchmark presents several noticeable advantages. First, we incorporate a broader range of prompt categories, ensuring diversity and representativeness in the prompt generation. Second, we introduce four rating dimensions, offering a more comprehensive assessment of sample quality compared to T³Bench. Although GPTEval3D employs more dimensions, it only provides preferences for a limited number of pairs. Third, to promote robust and unbiased scoring, we annotate all generated samples and recruit 21 subjects to rate 1,280 samples across four dimensions. Additionally, we apply comprehensive outlier detection to refine the MOS, reducing the impact of anomalous ratings. We will make the MOS publicly accessible, facilitating further validation and experimentation by other researchers.

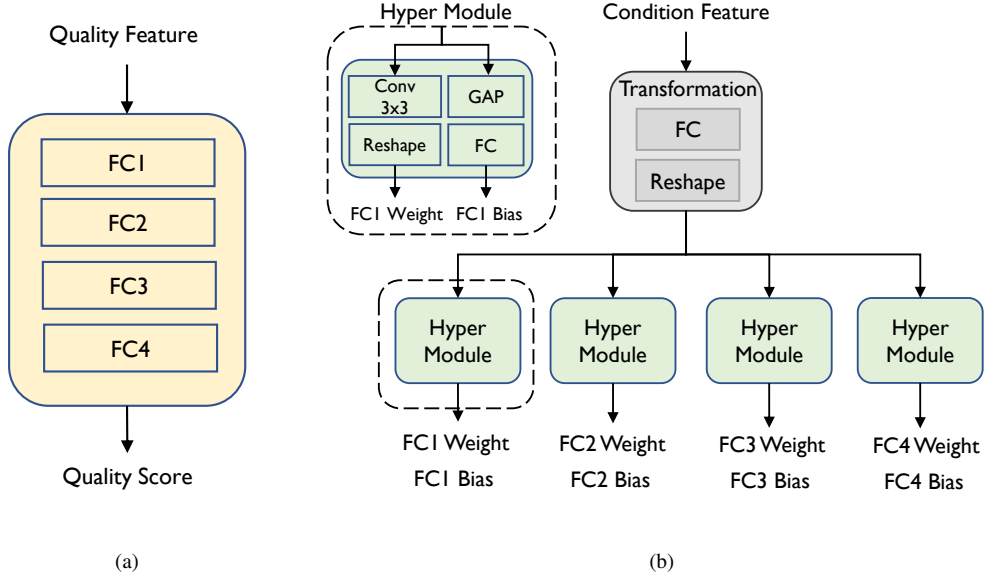


Figure S3. (a) Architecture of the mapping head; (b) Architecture of the hypernetwork.

C. More Details on Evaluator Implementation

C.1. Network Details

Utilization of Pre-trained Model. The used visual encoder in HyperScore is Vision Transformer [6] with 16×16 patch embeddings (namely ViT-B/16) in CLIP-Visual. The textual encoder is also the pre-trained transformer in CLIP-Textual. The visual, textual, and condition features all have a size of $D = 512$ while the quality feature has a size of $D_q = 224$.

Architecture of HyperNetwork and Mapping Head.

In the evaluator, we use a hypernetwork $\pi(\cdot)$ to generate the parameter weights for a mapping head $\psi(\cdot)$. We illustrate the network structure of $\pi(\cdot)$ and $\psi(\cdot)$ in Fig. S3. Seeing Fig. S3a, the mapping head contains four fully connected (denoted by FC1-FC4) layers and takes the quality feature as input to generate the quality score. The input sizes of four FC layers are 224, 112, 56, and 28 as shown in Tab. S2. To inject the dimension-related information into the mapping head, we use the hypernetwork shown in Fig. S3b to generate the weights and biases for FC layers. More specifically, the condition feature after transformation is fed into four independent hyper modules, and each hyper module will output the weight and bias for the corresponding FC layer in the mapping head. We also declare the feature size for the weight and bias generated of the FC1 layer in Tab. S2.

C.2. Loss Function

Given K evaluation dimensions, we finally obtain $\{\hat{q}_i\}_{i=1}^K$ as predictions. Denoting the subjective MOS as $\{q_i\}_{i=1}^K$, we

first define a regression loss as:

$$L_{reg} = \frac{1}{KB} \sum_{b=1}^B \sum_{i=1}^K (\hat{q}_i^b - q_i^b)^2, \quad (8)$$

where the superscript “ b ” denotes the b -th samples in a mini-batch with the size of B .

Considering that different evaluation dimensions have various focuses, to avoid learning homogeneous features, we define a feature disentangling loss for the condition features $\{f_c^i\}_{i=1}^K$:

$$L_{dis} = \frac{2}{K(K-1)} \sum_{i \neq j} \max(\epsilon, \cos(f_c^i, f_c^j)), \quad (9)$$

where $\cos(\cdot)$ denotes the cosine similarity between two features; ϵ represents the margin that controls the divergence among features and we set $\epsilon = 0$ in the implementation. By introducing L_{dis} , we can increase the discrepancy among different evaluation dimensions during the network training.

Finally, the overall loss function for training is defined as:

$$L = L_{reg} + \lambda L_{dis}, \quad (10)$$

where λ is the weighting factor, we simply set $\lambda = 1$.

C.3. Training Strategy

We train the proposed HyperScore on MATE-3D for 30 epochs with a batch size of 8. During the training and test-

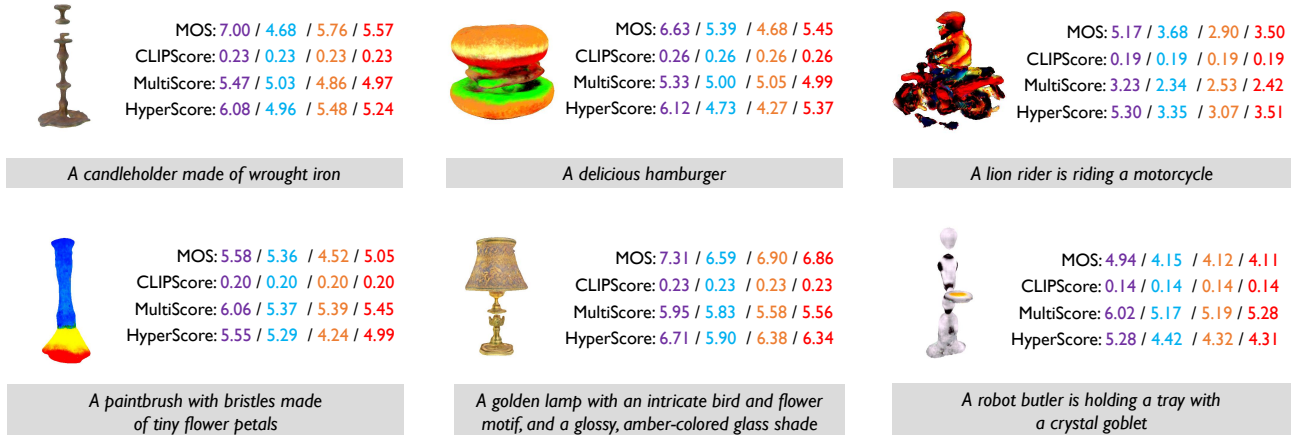


Figure S4. Additional exemplary samples with their MOSs and the predicted scores of different metrics. The four scores in each row denote alignment, geometry, texture, and overall quality, respectively.

Table S2. The feature size of each module in the hypernetwork and mapping head.

Module	Layer	Input Size	Output Size
Mapping Head	FC1 Layer	224	112
	FC2 Layer	112	56
	FC3 Layer	56	28
	FC4 Layer	28	1
Transformation	FC Layer	512	5,488
	Reshape	5,488	$112 \times 7 \times 7$
FC1 Weight Generation	3×3 Conv	$112 \times 7 \times 7$	$512 \times 7 \times 7$
	Reshape	$512 \times 7 \times 7$	224×112
FC1 Bias Generation	Global Avg Pool	$112 \times 7 \times 7$	$112 \times 1 \times 1$
	FC Layer	112	112

ing process, all rendered images are resized into the resolution of 224×224 . We use the Adam [24] optimizer with weight decay $1e - 4$. The learning rate is set separately as $2e - 6$ and $2e - 4$ for the pre-trained visual encoder and other parts (note that the textual encoder is frozen) and is reduced by a rate of 0.9 every 5 epochs.

D. Additional Experimental Results

D.1. Visualization

We provide additional qualitative samples in Fig. S4 for visualization. From the figure, we can observe that HyperScore presents more accurate predictions. In comparison, MultiScore usually assigns similar scores across different dimensions, making it challenging for users to determine which factor impacts visual perception more.

Furthermore, we visualize the weight maps used for con-

ditional feature fusion in Fig. S5. From the figure, we can observe that the weight maps differ across evaluation dimensions, demonstrating that the condition features contribute to distinguishing these dimensions. Meanwhile, we notice that the weight maps for the geometry evaluation have larger element values at the edges of objects, which may help to seize the shapes better. In comparison, the overall evaluation exhibits a more uniform distribution of the weight maps, probably because it needs to consider various factors during the evaluation process.

Finally, we present a qualitative analysis using a prevalent tool (*i.e.*, XGrad-CAM [7]) for network explanation. As illustrated in Fig. S6, the XGrad-CAM maps reflect what makes the network perform decisions for different evaluation dimensions. We observe that the XGrad-CAM maps exhibit different focus areas corresponding to changes in evaluation dimensions, which validates the effectiveness of the proposed conditional learning strategy. Notably, the XGrad-CAM maps related to the geometry evaluation pay more attention to the shape and structure of objects (*e.g.*, missing bones of the skeleton knight). In contrast, the texture and overall quality evaluations have a wider range of focus, likely because they require more appearance details to make decisions.

D.2. Additional Ablation Studies

Ablation Study for the Aggregation Strategy. We test the performance of HyperScore with different aggregation strategies between the visual and textual features. Except for the used element-wise multiplication (denoted by \odot), we choose two other strategies, *i.e.*, addition (denoted by $+$) and concatenation (denoted by \oplus). According to the results in Tab. S3, we can see that the element-wise multiplication performs best on all evaluation dimensions, and the

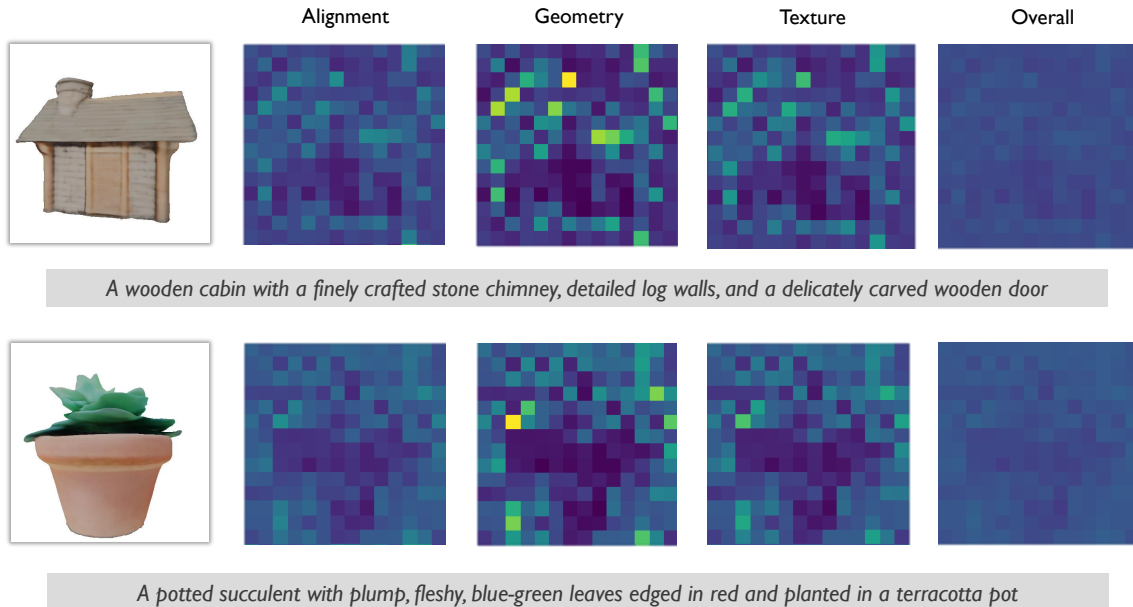


Figure S5. Visualization for the weight maps used for conditional feature fusion.

Table S3. Ablation study for the aggregation strategy between visual and textual features. Results of SRCC are reported.

Aggregation	Alignment	Geometry	Texture	Overall
$f_{v,c}^i + f_t^{eot}$	0.708	0.769	0.783	0.767
$f_{v,c}^i \oplus f_t^{eot}$	0.717	0.766	0.789	0.767
$f_{v,c}^i \odot f_t^{eot}$	0.739	0.782	0.811	0.792

addition and concatenation both provide relatively inferior performance, which justifies our choice for the aggregation strategy.

Ablation Study for the Viewpoint Count. To perform evaluation, we render textured meshes into $M = 6$ images from six perpendicular viewpoints (*i.e.*, along the positive and negative directions of the x, y, and z axes). We further test the performance of HyperScore under different M values to investigate the influence of the number of viewpoints and report the results in Tab. S4. Note that the corresponding camera locations of different M are declared in Tab. S5. From Tab. S4, it can be observed that as the M value increases, the performance initially improves and then decreases. The reason may be that increasing M provides more information for a better prediction when M is a small number. However, when M becomes large, the increase in M can affect performance to some extent due to information redundancy. Meanwhile, a larger M also incurs higher computational complexity. Therefore, to achieve the balance between performance and complexity, we consider

Table S4. Ablation study for the number of rendered viewpoints. Results of SRCC are reported.

M	Alignment	Geometry	Texture	Overall
4	0.716	0.755	0.790	0.766
6	0.739	0.782	0.811	0.792
9	0.737	0.780	0.810	0.790
12	0.724	0.784	0.805	0.784
16	0.724	0.784	0.805	0.784

Table S5. Camera locations of different view counts.

M	Elevation Angle	Azimuth Angle
4	$-60^\circ, 60^\circ$	$0^\circ, 180^\circ$
9	$-60^\circ, 0^\circ, 60^\circ$	$0^\circ, 120^\circ, 240^\circ$
12	$-60^\circ, 0^\circ, 60^\circ$	$0^\circ, 90^\circ, 180^\circ, 270^\circ$
16	$-60^\circ, -30^\circ, 30^\circ, 60^\circ$	$0^\circ, 90^\circ, 180^\circ, 270^\circ$
6	$(0^\circ, 0^\circ), (0^\circ, 90^\circ), (0^\circ, 180^\circ), (0^\circ, 270^\circ), (90^\circ, 0^\circ), (-90^\circ, 0^\circ)$	

$M = 6$ as a suitable choice.

Ablation Study for the Prompt Design. In our implementation, to obtain multiple condition features, we first transform the meta texts (*i.e.*, “alignment quality”, “geometry quality”, “texture quality”, “overall quality”) into text tokens and then insert them into the front of K learnable prompts with $L = 12$ tokens. Here we further explore the impact of L on the performance and illustrate the results in Fig. S7. From the figure, we see that HyperScore performs the best with $L = 12$. Short prompts may constrain the learning space, potentially leading to the loss of cru-

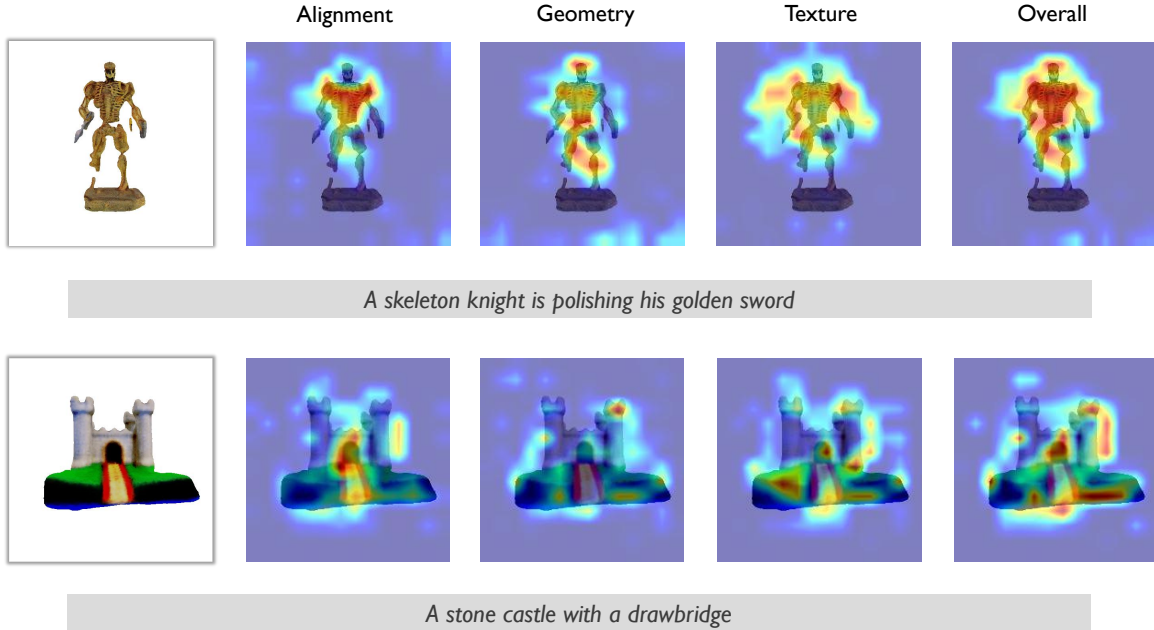


Figure S6. Visual explanations generated by XGrad-CAM for different evaluation dimensions.

cial information. Conversely, too long prompts might introduce unnecessary noise, which may obscure important information and degrade performance. Therefore, balancing the prompt length is critical to optimizing the metric performance.

We further replace these learnable prompts with fixed tags and test the performance of the case. Specifically, we define the tags for the four quality dimensions as:

- **Alignment:** “*quantity, attributes, position, location*”;
- **Geometry:** “*shape, size, hole, edge, surface*”;
- **Texture:** “*color, material, clarity, texture, contrast*”;
- **Overall:** “*quantity, attributes, position, location, shape, size, hole, edge, surface, color, material, clarity, texture, contrast*”.

The performance of the fixed tags is reported in Tab. S6, where we also report the performance of only using learnable tokens without the meta texts (denoted by “Learnable w/o meta”). We can observe that the learnable prompts with the meta texts outperform the fixed tags and alleviate the need for meticulous prompt design. Meanwhile, introducing the meta texts also benefits network optimization.

Ablation Study for the Loss Function. The proposed network is trained using the regression loss L_{reg} , and the feature disentangling loss L_{dis} . We evaluate the effect of each loss function and report the results in Table S7. From the table, we can see that only utilizing L_{reg} can also achieve remarkable performance while L_{dis} benefits the evaluations of all dimensions. Considering L_{dis} only measures the linear similarity between features, one pos-

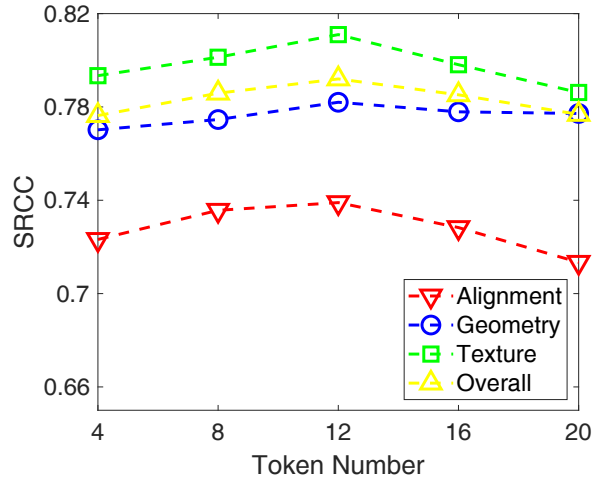


Figure S7. Performance comparison of the learnable prompt length.

sible avenue for further improvement is to minimize non-linear dependence between two features, such as mutual information.

D.3. Performance Comparison on Different Prompt Categories

In this section, we test the performance of different metrics on eight prompt categories and report the results in Tab. S8. For the metrics that need fine-tuning, we perform a leave-

Table S6. Ablation study for the prompt type. Results of SRCC are reported.

Prompt Type	Alignment	Geometry	Texture	Overall
Fixed	0.732	0.778	0.794	0.782
Learnable <i>w/o</i> meta	0.725	0.772	0.802	0.784
Learnable	0.739	0.782	0.811	0.792

Table S7. Ablation study for the loss function. Results of SRCC are reported.

Loss	Alignment	Geometry	Texture	Overall
L_{reg}	0.728	0.769	0.797	0.782
$L_{reg} + L_{dis}$	0.739	0.782	0.811	0.792

one-category-out evaluation, that is, testing on one category while training on the other seven categories, which can validate the generalization performance for unknown scenes. From the table, we have the following observations: i) HyperScore achieves the best performance on the four dimensions of almost all prompt categories, demonstrating its sensitivity to fine-grained scenes. In contrast, although some metrics work well on partial categories (*e.g.*, ImageReward on *Basic* and ViT+FT on *Spatial*), they may fail in other cases (*e.g.*, ImageReward on *Complex* and ViT+FT on *Basic*). ii) Almost all metrics perform better when evaluating single object generation than multiple object generation. This may be because these metrics do not model the specific relationships between objects well. iii) For the sub-categories of single and multiple object generation, most metrics perform best on *Basic* and *Grouped*, respectively. It is reasonable because the evaluation needs to incorporate more factors when measuring complex scenes and relationships, which presents challenges for the existing metrics.

D.4. Performance Comparison on Different Generative Methods

In this section, we test the performance of different metrics on eight generative methods and report the results in Tab. S9. For the metrics that require fine-tuning, we perform a leave-one-method-out evaluation, that is, testing on one generative method while training on other seven methods, which can validate the generalization performance for unknown generative methods. From the table, we have the following observations: i) HyperScore achieves the best performance on the four dimensions of almost all generative methods, demonstrating its generalization capability to new generative methods. In contrast, other metrics show inconsistent results across different methods. ii) Almost all fine-tuned metrics exhibit a noticeable decline in performance when evaluating the two recent methods, 3DTopia and One-2-3-45++. This may be because the two meth-

ods present different distortion patterns compared to other methods. More specifically, 3DTopia tends to generate a single object, leading to comparatively lower scores in multiple object generation. One-2-3-45++ tends to generate flatter geometric structures and blurry textures. These deformations, which are not seen during training, are very challenging for evaluation. In contrast, fine-tuned metrics work well on DreamFusion because many other methods inherit DreamFusion’s paradigm and generate similar patterns. Therefore, it is important to consider the generalization towards new generative methods when designing text-to-3D evaluators.

Table S8. Performance comparison (in terms of SRCC) of different evaluators on eight prompt categories.

Metric	Alignment							
	Basic	Refined	Complex	Fantastic	Grouped	Action	Spatial	Imaginative
CLIPScore	0.574	0.592	0.407	0.421	0.492	0.434	0.404	0.591
BLIPScore	0.640	0.520	0.479	0.423	0.590	0.476	0.577	0.540
Aesthetic Score	0.221	0.285	0.283	0.051	0.053	0.086	0.013	0.062
ImageReward	0.775	0.672	0.544	0.528	0.631	0.622	0.626	0.608
HPS v2	0.597	0.348	0.146	0.388	0.562	0.250	0.407	0.518
CLIP-IQA	0.058	0.144	0.082	0.127	0.042	0.006	0.086	0.114
ResNet50 + FT	0.625	0.603	0.582	0.601	0.548	0.429	0.562	0.475
ViT-B + FT	0.552	0.533	0.622	0.519	0.609	0.623	0.656	0.483
SwinT-B + FT	0.626	0.541	0.651	0.536	0.455	0.508	0.570	0.556
MultiScore	0.680	0.693	0.710	0.621	0.655	0.615	0.625	0.580
HyperScore	0.819	0.690	0.733	0.705	0.701	0.681	0.637	0.691
Metric	Geometry							
	Basic	Refined	Complex	Fantastic	Grouped	Action	Spatial	Imaginative
CLIPScore	0.575	0.570	0.438	0.404	0.496	0.503	0.479	0.602
BLIPScore	0.667	0.491	0.496	0.398	0.556	0.510	0.611	0.574
Aesthetic Score	0.244	0.279	0.268	0.053	0.164	0.041	0.088	0.028
ImageReward	0.790	0.545	0.558	0.467	0.532	0.588	0.585	0.600
HPS v2	0.617	0.355	0.218	0.364	0.504	0.334	0.423	0.544
CLIP-IQA	0.107	0.215	0.178	0.133	0.092	0.107	0.199	0.029
ResNet50 + FT	0.693	0.671	0.712	0.655	0.641	0.491	0.638	0.515
ViT-B + FT	0.692	0.643	0.752	0.568	0.704	0.598	0.700	0.552
SwinT-B + FT	0.720	0.618	0.738	0.579	0.558	0.559	0.637	0.622
MultiScore	0.733	0.753	0.802	0.670	0.727	0.625	0.723	0.634
HyperScore	0.862	0.745	0.838	0.742	0.776	0.690	0.736	0.738
Metric	Texture							
	Basic	Refined	Complex	Fantastic	Grouped	Action	Spatial	Imaginative
CLIPScore	0.620	0.616	0.472	0.442	0.514	0.519	0.528	0.631
BLIPScore	0.707	0.556	0.586	0.458	0.543	0.507	0.665	0.584
Aesthetic Score	0.218	0.310	0.306	0.108	0.257	0.053	0.108	0.030
ImageReward	0.800	0.597	0.596	0.510	0.505	0.606	0.626	0.618
HPS v2	0.620	0.359	0.217	0.370	0.508	0.376	0.464	0.584
CLIP-IQA	0.128	0.228	0.230	0.215	0.111	0.165	0.223	0.023
ResNet50 + FT	0.721	0.703	0.733	0.658	0.654	0.686	0.553	0.477
ViT-B + FT	0.702	0.682	0.782	0.619	0.721	0.692	0.668	0.603
SwinT-B + FT	0.747	0.617	0.770	0.598	0.580	0.624	0.666	0.652
MultiScore	0.776	0.778	0.843	0.671	0.735	0.695	0.747	0.691
HyperScore	0.880	0.792	0.852	0.745	0.807	0.761	0.746	0.732
Metric	Overall							
	Basic	Refined	Complex	Fantastic	Grouped	Action	Spatial	Imaginative
CLIPScore	0.590	0.587	0.441	0.433	0.497	0.519	0.473	0.621
BLIPScore	0.678	0.508	0.502	0.433	0.570	0.507	0.626	0.579
Aesthetic Score	0.244	0.295	0.305	0.056	0.166	0.053	0.059	0.021
ImageReward	0.793	0.588	0.572	0.504	0.569	0.606	0.616	0.617
HPS v2	0.623	0.347	0.200	0.380	0.530	0.376	0.427	0.537
CLIP-IQA	0.096	0.202	0.163	0.163	0.064	0.165	0.155	0.023
ResNet50 + FT	0.690	0.675	0.695	0.640	0.611	0.608	0.508	0.512
ViT-B + FT	0.670	0.640	0.739	0.567	0.664	0.679	0.613	0.552
SwinT-B + FT	0.710	0.598	0.732	0.572	0.519	0.590	0.620	0.616
MultiScore	0.734	0.748	0.811	0.665	0.699	0.656	0.694	0.643
HyperScore	0.865	0.760	0.841	0.750	0.759	0.730	0.717	0.756

Table S9. Performance comparison (in terms of SRCC) of different evaluators on eight generative methods.

Metric	Alignment							
	DreamFusion	Magic3D	SJC	TextMesh	Consistent3D	LatentNeRF	3DTopia	One-2-3-45++
CLIPScore	0.500	0.337	0.514	0.356	0.242	0.431	0.411	0.361
BLIPScore	0.550	0.390	0.520	0.443	0.337	0.527	0.502	0.337
Aesthetic Score	0.076	0.092	0.088	0.074	0.057	0.029	0.361	0.074
ImageReward	0.677	0.538	0.585	0.610	0.508	0.632	0.613	0.547
HPS v2	0.497	0.275	0.316	0.420	0.249	0.295	0.340	0.267
CLIP-IQA	0.223	0.163	0.040	0.179	0.023	0.122	0.094	0.137
ResNet50 + FT	0.689	0.508	0.450	0.530	0.430	0.401	0.259	0.222
ViT-B + FT	0.726	0.582	0.475	0.652	0.389	0.396	0.376	0.155
SwinT-B + FT	0.722	0.560	0.347	0.649	0.442	0.462	0.148	0.223
MultiScore	0.784	0.670	0.657	0.597	0.672	0.493	0.365	0.415
HyperScore	0.846	0.754	0.724	0.816	0.724	0.697	0.599	0.573
Metric	Geometry							
	DreamFusion	Magic3D	SJC	TextMesh	Consistent3D	LatentNeRF	3DTopia	One-2-3-45++
CLIPScore	0.511	0.323	0.493	0.343	0.226	0.418	0.360	0.269
BLIPScore	0.549	0.356	0.537	0.431	0.328	0.553	0.426	0.316
Aesthetic Score	0.159	0.156	0.088	0.051	0.015	0.005	0.452	0.367
ImageReward	0.665	0.461	0.588	0.552	0.433	0.555	0.503	0.421
HPS v2	0.506	0.299	0.311	0.429	0.252	0.346	0.309	0.331
CLIP-IQA	0.202	0.099	0.014	0.142	0.026	0.085	0.099	0.078
ResNet50 + FT	0.707	0.537	0.482	0.545	0.443	0.439	0.429	0.358
ViT-B + FT	0.743	0.563	0.582	0.629	0.375	0.466	0.546	0.215
SwinT-B + FT	0.729	0.529	0.382	0.602	0.434	0.525	0.369	0.184
MultiScore	0.741	0.620	0.595	0.585	0.581	0.446	0.588	0.418
HyperScore	0.821	0.717	0.703	0.773	0.657	0.708	0.683	0.653
Metric	Texture							
	DreamFusion	Magic3D	SJC	TextMesh	Consistent3D	LatentNeRF	3DTopia	One-2-3-45++
CLIPScore	0.502	0.406	0.509	0.393	0.259	0.434	0.384	0.258
BLIPScore	0.542	0.400	0.532	0.462	0.330	0.536	0.473	0.298
Aesthetic Score	0.141	0.122	0.095	0.020	0.003	0.047	0.450	0.356
ImageReward	0.671	0.489	0.573	0.568	0.435	0.535	0.543	0.420
HPS v2	0.516	0.295	0.330	0.450	0.266	0.307	0.367	0.307
CLIP-IQA	0.195	0.101	0.024	0.119	0.006	0.169	0.093	0.007
ResNet50 + FT	0.702	0.532	0.450	0.553	0.421	0.432	0.395	0.412
ViT-B + FT	0.735	0.606	0.572	0.636	0.392	0.483	0.492	0.220
SwinT-B + FT	0.734	0.524	0.374	0.617	0.459	0.519	0.340	0.171
MultiScore	0.755	0.634	0.603	0.598	0.593	0.472	0.610	0.448
HyperScore	0.823	0.736	0.694	0.775	0.702	0.694	0.613	0.623
Metric	Overall							
	DreamFusion	Magic3D	SJC	TextMesh	Consistent3D	LatentNeRF	3DTopia	One-2-3-45++
CLIPScore	0.506	0.342	0.517	0.362	0.208	0.428	0.399	0.330
BLIPScore	0.548	0.380	0.553	0.443	0.300	0.543	0.473	0.347
Aesthetic Score	0.118	0.149	0.066	0.005	0.001	0.029	0.434	0.242
ImageReward	0.678	0.504	0.602	0.577	0.440	0.572	0.555	0.517
HPS v2	0.507	0.291	0.337	0.436	0.241	0.318	0.336	0.322
CLIP-IQA	0.206	0.135	0.023	0.156	0.005	0.111	0.104	0.028
ResNet50 + FT	0.703	0.543	0.470	0.535	0.525	0.432	0.357	0.302
ViT-B + FT	0.731	0.597	0.561	0.635	0.388	0.439	0.460	0.190
SwinT-B + FT	0.733	0.567	0.363	0.639	0.441	0.499	0.297	0.230
MultiScore	0.769	0.659	0.635	0.597	0.613	0.451	0.508	0.444
HyperScore	0.839	0.745	0.730	0.794	0.698	0.718	0.638	0.634



Please assist us in creating a set of text prompts for text-to-3D generation. To ensure diversity and comprehensiveness in the prompts, the content should focus on the following four aspects. Here, we provide the definitions below:

1. Object categories:

- Living Beings: Humans, animals, mythical creatures, insects, aquatic life
- Plants: Trees, flowers, bushes, grass, aquatic plants
- Buildings and Structures: Houses, skyscrapers, bridges, tunnels, castles
- Vehicles: Cars, bikes, planes, boats, spacecraft
- Furniture: Chairs, tables, sofas, shelves, beds
- Electronics: Phones, computers, cameras, kitchen appliances
- Household Items: Utensils, decor, tools, containers
- Clothing and Accessories: Dresses, shoes, jewelry, hats, bags
- Abstract Objects: Geometric shapes, artistic sculptures
- Natural Elements: Fire, water, rocks, clouds
- Food and Beverages: Fruits, vegetables, dishes, drinks

2. Geometry properties:

- Volume: Specify if the object is hollow, solid, porous, or layered.
- Symmetry: Define if the object should be symmetrical, asymmetrical, or radially symmetrical.
- Contours: Indicate if the contours should be smooth, jagged, irregular, or undulating.
- Internal Structures: State if the inside should be empty, compartmentalized, or multi-layered.
- Shape: Mention specific geometric shapes that should be part of or inspire the object, e.g., cone, cylinder, sphere.
- Size: Small, medium, large, specific dimensions

3. Appearance properties:

- Colors: Specific colors, patterns, gradients
- Materials: Wood, metal, glass, fabric, stone
- Textures: Smooth, rough, furry, scaly
- Finish: Glossy, matte, translucent, opaque
- State: New, old, worn, pristine

4. Object interaction:

- Spatial relation: the orientation or movement involved in the interaction, describing where the subject and object are in relation to each other. e.g. toward, above, below, near to, on the left/right/top/bottom of
- Action relation: Specific verbs representing interactions between subjects and objects, e.g. wear, watch, speak to, hold, run, jump, kiss, sit on, stand on, walk with, play with

Then, we will give you some more tips and requirements for the prompt creation. Here, we will present different categories for single object generation and multiple object generation, respectively.

For single object generation, we define four categories:

1. **Basic:** descriptions about a single object without detailed geometry or appearance details, where some global properties (e.g., color, shape, material) could be included. Here are examples: "A green apple", "A humanoid robot", "A square table", "A wooden chair".
2. **Refined:** descriptions about a single object with one simple specification of the geometry or appearance details. Here are examples: "A photo of a black bird", "A yellow rubber duck has only one foot", "A plastic cup with a printed logo", "An imperial state crown of England".
3. **Complex:** descriptions about a single object with more than two detailed specifications of geometry or appearance details. Here are examples: "A brown teddy bear, fur matted, one eye missing", "A turtle standing on its hind legs, wearing a top hat and holding a cane", "An oversized, porous, sphere-shaped birdcage, made of woven golden wires".
4. **Fantastical:** descriptions about a single object with high creativities that are not, or are generally unlikely to be, found in the real world. Here are examples: "A frog with a translucent skin displaying a mechanical heart beating", "A squirrel-octopus hybrid", "A white cat has three tails, made of white, purple and black crystals", "A tiger dressed as a doctor".

For multiple object generation, we define four categories:

1. **Grouped:** descriptions about multiple objects without interactions, where some global properties (e.g., color, shape, material) could be included. Here are examples: "A delicious hamburger and a green apple", "A red pig and a huge drum", "A round table and a square chair".
2. **Action:** descriptions about multiple objects with interaction about action relations, where some geometry or appearance details could be included. Here are examples: "A humanoid robot with a top hat is playing the cello", "A black cat with white feet is sleeping peacefully beside a carved pumpkin", "A dog is eating a red apple with its tail raised".
3. **Spatial:** descriptions about multiple objects with interactions about spatial relations, where some geometry or appearance details could be included. Here are examples: "A red apple on a round ceramic plate", "A strong football player wearing a number seven jersey next to a blue soccer", "A blue rose in a crystal, symmetrical vase".
4. **Imaginative:** descriptions about multiple objects with interactions, where objects or interactions are not, or are generally unlikely to be found in the real world. Here are examples: "A panda with a wizard hat is reading a newspaper", "A ghost is eating a golden apple", "A lion wearing a crown is painting with a glowing paintbrush", "A raccoon astronaut is holding his helmet".

Try to understand the requirement first, before I provide some more information.



Got it! You've outlined a detailed framework with distinct categories, geometry and appearance properties, and types of interactions for both single and multiple object generation. Here's a quick summary to confirm my understanding of what you need:

- Object Categories:** Diverse sets of real and abstract objects—ranging from living beings to food.
 - Geometry Properties:** Details like symmetry, contours, shape, and volume to define the structural features.
 - Appearance Properties:** Including colors, materials, textures, and finish to dictate the look and feel of objects.
 - Object Interaction:** Focus on spatial and action-related interactions between objects, especially for multiple object generation.
- Then, the challenges break down as follows:

Single Object Generation:

- Basic:** Simple object descriptions with minimal detail.
- Refined:** One additional property for a bit more complexity.
- Complex:** Multiple geometry or appearance properties for detailed descriptions.
- Fantastical:** Creative, unreal objects that may blend features or stretch reality.

Multiple Object Generation:

- Grouped:** Multiple objects without interaction.
- Action:** Interactions involving actions, like movement or usage.
- Spatial:** Objects with spatial relations to each other.
- Imaginative:** Unreal interactions or fantastical scenes.

This structure ensures a diverse and comprehensive prompt set, with various levels of detail and creativity across single and multiple object descriptions. I'm ready for the next steps, such as requirements for the prompt creation. Please provide the additional information or tips you mentioned.

Figure S8. Examples of guiding GPT-4 for automatic prompt generation. (Part 1/2)

Please create 100 "Basic" prompts about "single object generation" within 10 words. Do not describe the environment. Please make sure that the prompt you provided has enough diversity and comprehensiveness, and that the format is similar to my example.



Here are 100 "Basic" prompts about a single object, each within 10 words, ensuring a wide range of categories and diversity:

1. A striped zebra
2. A green pepper
3. A brown leather belt
4. A glowing light bulb
5. A blue vase
6. A round stool
7. A wooden boat
8. A white wedding dress
9. A round gold coin
10. A silver spoon
11. A wooden dining table
12. A yellow pencil
13. A purple notebook
14. ...
-
100. A delicious hamburger

These prompts span a variety of categories, including clothing, accessories, household items, vehicles, and natural elements, ensuring coverage of different forms, materials, and textures.

Please create 100 "Spatial" prompts about "multiple object generation" within 20 words. Do not describe the environment. Please make sure that the prompt you provided has enough diversity and comprehensiveness, and that the format is similar to my example.



Here are 100 "Spatial" prompts about multiple objects, each within 20 words, focusing on spatial relationships between objects with diversity and clarity:

1. A red apple on a white ceramic plate
2. A black hat hanging on a brass hook
3. A glass teapot next to a porcelain cup
4. A golden key inside a brown leather pouch
5. A blue backpack under a wooden bench
6. A silver spoon resting on a folded napkin
7. A cat sitting next to a pair of shoes
8. A guitar leaning against a wooden chair
9. A clock above a wooden bookshelf
10. A pair of sunglasses on top of a magazine
11. A candle placed inside a glass jar
12. A handwoven basket filled with a ripe peach
13. A set of dice beside a deck of cards
14. ...
-
100. A small cactus inside a clay pot

These prompts ensure spatial relationships between objects are clear, diverse, and easy to visualize while maintaining a compact, simple structure.

Please create 100 "Imaginative" prompts about "multiple object generation" within 20 words. Do not describe the environment. Please make sure that the prompt you provided has enough diversity and comprehensiveness, and that the format is similar to my example.



Here are 100 "Imaginative" prompts about multiple objects, each within 20 words, ensuring diversity, creativity, and intriguing interactions between objects:

1. A giraffe wearing sunglasses plays chess with a robot
2. A dragon sipping tea from a porcelain cup
3. A violin floating next to a glowing crystal ball
4. A penguin in a tuxedo is conducting an orchestra with a baton
5. A ghost riding a bicycle with a pumpkin helmet
6. A knight polishing his sword while a cat reads a map
7. A frog wearing boots and holding an umbrella
8. A unicorn carrying a glowing lantern on its horn
9. A lion rider is riding a motorcycle
10. A shark with a crown is holding a golden trident
11. A bear astronaut is planting a flag with a paw print
12. A phoenix with flaming wings is carrying a silver lantern
13. A raccoon detective is studying a map under a magnifying glass
14. ...
-
100. A dog wearing backpack is walking on a rainbow

These imaginative prompts feature whimsical, surreal interactions between objects and creatures, maintaining variety and unexpected combinations for creativity in 3D generation.

Figure S9. Examples of guiding GPT-4 for automatic prompt generation. (Part 2/2)



	DreamFusion	Magic3D	SJC	TextMesh	3DTopia	Consistent3D	LatentNeRF	One2-3-45++
Basic	A green pepper							
								
	8.74/8.39/7.39/8.00	8.89/8.73/7.67/8.43	5.00/3.28/2.80/3.71	9.53/8.95/8.44/8.90	6.41/5.42/5.81/5.74	5.74/5.00/4.72/4.90	3.56/2.10/2.82/2.58	8.85/8.76/7.88/8.47
Refined	A cactus with a blooming flower							
								
	6.58/5.45/5.57/5.76	7.58/5.63/5.72/6.10	6.82/4.89/4.44/5.32	6.17/5.10/5.12/5.53	6.41/5.42/5.81/5.74	3.16/2.67/2.50/2.62	7.00/6.41/5.53/6.11	6.89/4.94/4.75/5.33
Complex	A blue jacket with silver buttons, fur lining on the collar, and a tear on the right sleeve							
								
	4.89/4.17/4.28/4.29	7.00/6.89/6.75/7.05	1.06/1.19/1.29/1.11	7.26/6.75/6.78/7.00	6.11/6.00/5.55/5.76	5.56/4.90/4.94/4.95	2.63/2.06/2.05/1.95	6.79/7.33/7.00/7.10
Fantastical	A house shaped like a giant teapot, complete with handle and spout							
								
	4.89/5.06/4.70/4.38	4.42/4.50/3.44/3.76	4.89/3.28/3.39/3.48	4.89/5.47/3.94/4.29	6.33/6.06/5.10/5.68	5.11/5.47/4.61/4.57	3.76/2.58/2.94/2.58	6.35/6.42/6.38/6.00
Group	A green cactus and a glass bottle							
								
	5.12/6.00/6.13/5.47	5.90/7.88/7.59/6.95	5.89/5.63/4.85/5.20	5.42/7.00/6.80/5.90	4.24/4.19/4.45/4.21	4.90/4.41/4.29/4.16	3.53/2.68/3.06/2.84	4.32/5.32/5.76/4.86
Action	A duck is chasing a yellow ball with its wings flapping							
								
	5.94/5.47/5.50/5.11	6.05/4.06/3.89/4.33	5.16/3.73/3.24/3.86	4.21/3.50/3.78/3.52	1.58/1.58/1.78/1.38	3.89/3.58/3.67/3.48	6.86/4.75/4.90/5.53	7.61/6.47/6.25/6.55
Spatial	A polished silver bell resting on a wooden stand							
								
	6.68/6.50/5.61/6.24	7.00/6.78/6.39/6.48	4.41/2.84/2.81/3.16	7.11/7.21/6.89/7.00	4.38/4.95/5.50/4.50	5.81/5.44/4.65/5.26	5.06/3.47/3.56/3.79	7.63/8.00/8.00/7.86
Imaginative	A mermaid is holding a white conch shell							
								
	7.47/6.05/5.33/6.10	7.11/5.89/5.90/6.48	5.79/3.55/2.95/3.67	5.53/4.17/3.95/4.52	2.79/2.89/3.05/2.60	2.47/1.91/2.43/1.76	6.95/5.83/4.74/6.05	7.63/6.22/5.39/6.29

Figure S10. More results of eight generative methods for eight categories. The scores below each sample denote alignment, geometry, texture, and overall quality, respectively.